血清非存在下における
ヒト歯髄細胞の分離と幹細胞特性評価
～臨床的細胞治療に向けた実践的無血清培養法の確立～

望月　真衣

Establishment of xenogeneic serum-free culture methods for handling dental pulp stem cells using clinically oriented *in vitro* and *in vivo* conditions

Mai MOCHIZUKI

日本歯科大学大学院生命歯学研究科歯科基礎系専攻
（指導：生命歯学部発生・再生医科学講座　中原　貴　教授）
The Nippon Dental University, Graduate School of Life Dentistry at Tokyo
(Supervisor: Prof. Taka NAKAHARA, School of Life Dentistry at Tokyo, Department of Developmental and Regenerative Dentistry)

（2018 年 1 月）

この論文の内容は、次の形式で公表する。

論文題名：Establishment of xenogeneic serum-free culture methods for handling dental pulp stem cells using clinically oriented *in vitro* and *in vivo* conditions.

機関名：BioMed Central

雑誌名：Stem Cell Research & Therapy

著者名：Mai MOCHIZUKI and Taka NAKAHARA

本論文を望月真衣の博士（歯学）学位論文として提出することを

承認します。

中原　貴　　㊞

Abstract

Background: Currently, *ex vivo* handling of stem cells, including transport after harvest and therapeutic preparation, is generally done in culture media containing fetal bovine serum (FBS), which promotes cell attachment, proliferation, and differentiation. However, because of safety concerns associated with the use of FBS, including potential transmission of zoonotic agents and transplant rejection because of the incorporation of foreign proteins into the stem cells, there is a need for xenogeneic serum-free culture media for clinical handling of stem cells.

Methods: Dental pulp stem cells (DPSCs) were derived from wisdom teeth donated by eight healthy volunteers and cultured in xenogeneic serum-free culture medium (XFM) or xenogeneic serum-containing medium (SCM). Cells were subjected to morphological, proliferation, karyotype, differentiation, marker expression, cryopreservation, and cytotoxic susceptibility analyses *in vitro*, as well as transplantation *in vivo*.

Results: In primary culture, XFM cells showed lower adhesion and slightly different morphology, although single-cell size was similar to that of SCM cells. XFM cells exhibited typical mesenchymal stem cell (MSC) characteristics *in vitro* and *in vivo*, including marker gene/protein expression, trilineage differentiation potential, and hard, osteo-dentin tissue formation. Additionally, XFM cells maintained a normal karyotype *in vitro* and non-tumorigenic potential *in vivo*; however, XFM cells were more susceptible to H_2O_2 and UV cytotoxic stimuli. XFM cells formed a multilayered structure showing excessive cell death/division in contrast to the monolayered structure of SCM cells when

reaching over-confluence. In over-confluent XFM cells, proliferation was disrupted, and these cells could not be subcultured. DMSO-free cryopreserved XFM cells yielded similar results in all above experiments.

Conclusions: This study is the first reporting successful isolation and expansion of an MSC population from donor-derived tissue (dental pulp) under xenogeneic serum-free culture conditions, as well as the application of cryopreservation, using a research strategy based on clinically oriented *in vitro* and *in vivo* experiments.

Keywords: Dental pulp stem cells, Xenogeneic serum-free culture, Cell isolation, Stem cell characterization, Chromosomal stability, Cytotoxic susceptibility, *In vivo* transplantation, Cryopreservation, Cell cycle, Apoptosis

Background

Various somatic stem cell-based therapies involving cell isolation, expansion, and application for treatment have been developed, with part of these subsequently introduced into clinical practice [1, 2]. The development and application of a novel cell therapy requires *ex vivo* manipulation and therapeutic preparation of autologous stem cells [3–5]. Therefore, ensuring steady supplies of stem cells of various types and both quality and safety controls for the cells are essential for their wide application in stem cell-based tissue engineering and regenerative medicine [6, 7].

Mesenchymal stem cells (MSCs) isolated from dental pulp tissue of extracted teeth, which are generally discarded after dental treatments, represent autologous stem cell candidates for future cell therapies. Dental pulp stem cells (DPSCs) possess extensive proliferation ability, which is superior to that of iliac bone-marrow-derived MSCs [8, 9], and multipotency into a variety of cell lineages, such as osteoblasts, odontoblasts, adipocytes, chondrocytes, neurons, endothelial cells, myocytes, and hepatocytes *in vitro* [8–15]. Moreover, *in vivo* studies reported the effective application of DPSCs in several animal models of systemic diseases [16–19]. More recently, clinical studies reported the therapeutic use of DPSCs for bone augmentation in tooth-extraction defects [20] and for dental pulp regeneration in caries-affected, pulpectomized teeth [21]. Therefore, DPSCs are currently regarded a valuable, promising MSC type among somatic stem cells with clinical potential.

Fetal bovine serum (FBS) is generally added to culture media used for MSC isolation and expansion *in vitro*. The identified and unidentified contents of FBS facilitate various cell behaviors, such as cell attachment, proliferation, and differentiation, during

cell culture *ex vivo*. However, there are several safety concerns for clinical application of MSCs expanded *ex vivo* with FBS, including potential risks of immune/allergic reactions and transmission of harmful agents, such as prions, viruses, or zoonotic microorganisms, to the host. Moreover, proteins and peptides within FBS are believed to be incorporated into the cultured cells and subsequently transferred into the host through the cell-transplantation process, resulting in the rejection of transplanted cells [22, 23]. Hence, recent studies reported the development and application of xenogeneic serum-free culture media using several MSC types for the purpose of clinical use [24–26].

Although several FBS-free culture media are commercially available, it is widely accepted that the use of FBS is essential in transporting harvested tissue samples to the laboratory and when isolating MSCs in primary culture. However, culturing primary cells in conventional FBS-containing medium even once raises the aforementioned safety concerns. In the current study, we thoroughly investigated the isolation and expansion of DPSCs under FBS-free culture conditions, as well as the application of cryopreservation, using a research strategy based on clinically oriented *in vitro* and *in vivo* experiments. The aim of this study was to establish practical and reliable methods for handling DPSCs under xenogeneic serum-free culture conditions to enhance clinical application of donor-derived MSCs.

Methods

Isolation and expansion of DPSCs using FBS-free culture medium

Wisdom teeth were donated by eight healthy volunteers aged 20 to 37 years. The teeth were transported at 4°C in FBS-free basic culture medium comprising Dulbecco's modified Eagle's medium/Ham's nutrient mixture F12 (DMEM/F12), 100 μM glutamate, 0.1% MEM non-essential amino acids, 50 U/mL penicillin, 50 μg/mL streptomycin, and 0.25 mg/mL Fungizone (all from Thermo Fisher Scientific, Waltham, MA, USA). The collection of dental pulp tissue from extracted teeth and DPSC isolation were performed as previously described [8]. Briefly, the dental pulp tissue harvested from the teeth was minced and digested in a solution containing 3 mg/mL collagenase type I (Merck KGaA, Darmstadt, Germany) and 4 mg/mL dispase (Wako Pure Chemical Industries, Osaka, Japan) for 1 h at 37°C. After passing the cell suspension through a 70-μm cell strainer, the single-cell suspension was equally divided for cultivation in two types of culture media as follows: xenogeneic serum-free culture medium (XFM; PRIME-XV® MSC Expansion XSFM; Irvine Scientific, Santa Ana, CA, USA) and the aforementioned basic culture medium supplemented with 15% FBS, designated as xenogeneic serum-containing medium (SCM). The culture dishes/plates for XFM cultivation were pre-coated with PRIME-XV® human fibronectin (Irvine Scientific) in primary and subsequent cell cultures according to manufacturer recommendations. Cell cultures were maintained at 37°C in a humidified atmosphere containing 4.7% carbon dioxide in air, and both culture media were changed every 3 or 4 days. At 80% confluence, the cultured cells were detached using 0.25% trypsin (Becton Dickinson, Franklin Lakes, NJ, USA)/0.02% ethylenediaminetetraacetic acid (EDTA; Dojindo, Kumamoto, Japan) and

were subcultured at 5×10^3 cells/cm^2 in 60-mm culture dishes (Thermo Fisher Scientific). Cells at passage 3 or 4 were used for experiments, except for karyotype analysis (passage 10). All experiments were repeated independently at least three times.

Dimethyl sulfoxide (DMSO)-free cryopreservation of DPSCs

Part of the cells subcultured in XFM ("XFM cells") at passage 1 were stored in DMSO-free cryopreservation medium (CryoScarless® DMSO-free; BioVerde, Kyoto, Japan), at −80°C. After 1 to 3 months, the cryopreserved XFM cells were recovered and cultured until passage 3, followed by characterization.

Cell morphological and morphometric analyses

To evaluate subconfluent cells under the culture (adherent) condition, XFM and SCM cells were seeded at 5×10^3 cells/cm^2 into 60-mm culture dishes and cultured until subconfluence. Cells were fixed with 4% paraformaldehyde (PFA) and permeabilized with 1% Triton X-100 for 10 min. After washing with calcium- and magnesium-free phosphate-buffered saline (PBS), the cells were stained F-actin with Phalloidin-iFluor 488 conjugate (AAT Bioquest, Sunnyvale, CA, USA) and mounted with Vectashield hard-set mounting medium containing 4′,6-diamidino-2-phenylindole (DAPI; Vector Laboratories, Burlingame, CA, USA). Five hundred cells were randomly selected under a Biorevo BZ-9000 microscope (Keyence, Osaka, Japan), and the adhesive area of each cell was measured using image analysis software (BZ-H2A; Keyence).

To evaluate cells under floating (non-adherent) conditions, XFM and SCM cells at subconfluence were detached by trypsin-EDTA treatment and fixed with 4% PFA. After washing with PBS, the cells were analyzed by measuring the transmitted light using PERFLOW® Sort V-4cTS2L-D (Furukawa, Chiba, Japan). The data were analyzed with

FlowJo software (version 10; TreeStar, Ashland, OR, USA).

To observe fine cell morphology, both types of cells were seeded at 5×10^3 cells/cm^2 into 35-mm glass-bottom culture dishes (Greiner Bio-One, Frickenhausen, Germany). The cells were fixed with 4% PFA at confluence or over-confluence and stained with Phalloidin-iFluor™ 488 conjugate and DAPI as described. Fluorescence and phase-contrast images were obtained by using an inverted fluorescence microscope (IX71; Olympus, Tokyo, Japan). For three-dimensional (3D) analysis of confluent cell cultures, Z-stack images were obtained with a confocal laser-scanning microscope (LSM 700; Carl Zeiss, Oberkochen, Germany), and 3D images were reconstituted from the Z-stack data with image analysis software (IMARIS version 7.11; Bitplane, Zurich, Switzerland).

Cell proliferation analyses

XFM and SCM cells (5×10^3 cells/cm^2) were seeded into 12-multiwell plates (SumitomoBakelite, Tokyo, Japan) and cultured for 14 days. The cultured cells were detached using trypsin-EDTA and routinely counted in triplicate with a hemocytometer every 2 days. Population doubling time (PDT) was calculated using the following formula:

$$\mathrm{PDT} = \frac{(t - t_0)\log_2}{\log(N - N_0)}$$

where t equals time (hours), N equals the number of cells, and N_0 and N represent the number of cells at t_0 and t, respectively.

Electrochemiluminescence immunoassay (ECLIA)

The levels of carcinoembryonic antigen (CEA), squamous cell carcinoma antigen (SCC),

and neuron-specific enolase (NSE), which are common neoplastic/tumorigenic transformation markers, within conditioned media collected from XFM and SCM cultures on day 14 were measured by automated ECLIA in a commercial laboratory (SRL, Tokyo, Japan).

Karyotype analysis

Chromosomal G-band analysis of XFM and SCM cells at passage 10 was performed at the Nihon Gene Research Laboratories (Sendai, Japan). Briefly, subconfluent cells were subjected to karyotype analysis, and Giemsa-stained cell metaphase spreads were prepared according to standard cytogenetic methods and randomly selected for analysis. Chromosome numbers were counted in 50 metaphase spreads, and G-banding patterns were assessed in 20 metaphase spreads.

Cell-surface-marker expression analysis by flow cytometry

Subconfluent cells were collected with trypsin-EDTA and fixed with 4% PFA for 20 min at room temperature. After washing with PBS, the fixed cells were labeled with fluorescein isothiocyanate-conjugated antibodies against human CD14 (clone M5E2), CD90 (clone 5E10), and CD105 (clone 266) (Becton Dickinson); CD34 (clone 581) and CD44 (clone J.173) (Beckman Coulter, Fullerton, CA, USA); STRO-1 (clone STRO-1; Santa Cruz Biotechnology, Dallas, TX, USA); and phycoerythrin-conjugated mouse immunoglobulin (Ig) G1 (clone MOPC-21; Becton Dickinson). Flow-cytometric analysis was performed using a Guava^{TM} EasyCyte HT system and Guava^{TM} Express Plus software (version 2.7; Merck KGaA).

Reverse transcription polymerase chain reaction (RT-PCR)

To detect the gene-expression profiles of MSC, osteogenic, and adipogenic markers, total RNA was extracted from XFM and SCM cultures at passage 3. To explore the time-course expression of apoptosis- and cell cycle-related genes, XFM and SCM cells (5×10^3 cells/cm^2) were seeded into 12-multiwell plates and cultured for 14 days. Total RNA was extracted from the cultures every 2 days from days 6 to 14. RT-PCR was performed according to our previous report [27]. The semiquantitative densitometric analysis of the observed signals was performed using ImageJ software (version 1.48; National Institutes of Health, Bethesda, MD, USA) and expressed as a ratio to β-actin signal intensity. Primer sequences and PCR conditions are shown in Table 1.

***In vitro* multilineage differentiation**

In vitro multilineage differentiation experiments (osteogenic, adipogenic, and chondrogenic) were performed according to our previous report [27]. Briefly, for osteogenic and adipogenic differentiation, XFM and SCM cells were seeded at 1×10^5 cells/well in 6-well plates (SumitomoBakelite). Both types of cells were cultured in osteogenic induction medium: α-modified minimal essential medium (α-MEM; Wako Pure Chemical) containing 10% FBS, 10 nM dexamethasone (Merck KGaA), 10 mM β-glycerophosphate (Merck KGaA), and 100 μM L-ascorbate-2-phosphate (Wako Pure Chemical); or adipogenic induction medium: α-MEM containing 10% FBS, 0.5 mM 3-isobutyl-l-methylxanthine (Merck KGaA), 0.5 μM hydrocortisone (Wako Pure Chemical), and 60 μM indomethacin (Merck KGaA). As a control, the cells were cultured in α-MEM supplemented with 10% FBS lacking the osteogenic or adipogenic supplements. After 4 weeks of differentiation, the mineralized deposits were visualized by alizarin red S staining, and intracellular accumulation of lipid droplets was visualized by oil red O

staining. For chondrogenic differentiation, approximately 1×10^6 cells were centrifuged at 150 *g* for 5 min to form a pellet. The pellets were cultured in chondrogenic induction medium: DMEM/F12 containing 10% FBS, 10 ng/mL of transforming growth factor-β1 (Peprotech, Oak Park, CA, USA), 1% ITS+1 supplement (Merck KGaA), and 50 mM L-ascorbate-2-phosphate (Wako Pure Chemical). After 4 weeks of differentiation, the pellets were fixed in 4% PFA, embedded in paraffin, and sectioned at a thickness of 5-μm for histological analysis. Chondrogenic differentiation was determined by staining with alcian blue (Merck KGaA) and safranin-O (Waldeck GmbH & Co. KG, Münster, Germany) and by immunohistochemistry. The rabbit polyclonal anti-type II collagen primary antibody (1:50; Santa Cruz Biotechnology) was used. The sections were examined using a Biorevo BZ-9000 microscope (Keyence).

***In vitro* assessment of cell damage induced by extrinsic cytotoxic stimuli**

To evaluate cell susceptibility to extrinsic stimuli, XFM and SCM cells (5×10^3 cells/cm^2) were seeded into 12-multiwell plates and treated with 1 μM staurosporine (Wako Pure Chemical Industries) or 100 μM hydrogen peroxide (H_2O_2; Wako Pure Chemical Industries) for 6 hours at 37°C or were exposed to ultraviolet (UV) radiation using a UV transilluminator (UVP, Upland, CA, USA) for 30 minutes at room temperature. Staurosporine, which is a known chemical inducer of apoptosis, was used as a positive control for cell-damage induction. Cell damage was evaluated by flow cytometry using an Annexin V/propidium iodide (PI) system described previously [28], with minor modifications. Briefly, the treated cells were stained with 100 μL of Guava Nexin® reagent (Merck KGaA) for 20 min at room temperature in the dark and subjected to flow cytometry in the Guava™ EasyCyte HT system equipped with Guava InCyte software (Merck KGaA). The data were analyzed with FlowJo software (TreeStar). Annexin V-

positivity and PI-negativity indicated the fraction of early apoptotic cells and Annexin V/PI-double positivity indicated the fraction of late-apoptotic cells. We considered that both fractions represented damaged cells [28]. The results were expressed as the ratio of the number of damaged cells to the number of non-damaged cells.

In vivo transplantation and histological evaluation

DPSCs expanded using XFM or SCM were subcutaneously transplanted under the dorsal skin of 6-week-old female nude mice (BALB/C-nu/nu; Nihon Clea, Tokyo, Japan). The preparation of cell-loaded hydroxyapatite/β-tricalciumphosphate (HA) constructs and the transplantation procedure were performed according to our previous report [28]. HA constructs alone were included as a control. All constructs were collected 16 weeks after transplantation. The samples were fixed with 4% PFA, decalcified, embedded in paraffin, and sectioned serially at 5-μm thickness [29]. The serial sections were subjected to hematoxylin and eosin (HE), Masson's trichrome (MT), and immunohistochemical staining. Immunohistochemistry was conducted as previously described [27, 28]. Mouse monoclonal anti-human-specific vimentin (1:10,000; Merck KGaA) and rabbit polyclonal anti-dentin sialoprotein (DSP; 1:200; Santa Cruz Biotechnology) were used as primary antibodies. All slides were examined using a Biorevo BZ-9000 microscope (Keyence).

Terminal deoxynucleotidyl transferase-mediated deoxyuridine triphosphate nick-end labeling (TUNEL) staining

To examine apoptotic cells within over-confluent monolayer/multilayer cultures and cell aggregates derived from subcultured over-confluent XFM cells, TUNEL staining was performed. Briefly, over-confluent cultures and cell aggregates were fixed in 4% PFA,

embedded in paraffin, and sectioned at 5-μm thickness. Deparaffinized sections were subjected to TUNEL staining according to manufacturer instructions (Roche Diagnostics, Mannheim, Germany). DNA fragmentation of apoptotic cells was observed using a Biorevo BZ-9000 microscope (Keyence).

Detection of apoptotic cells by flow cytometry with Annexin V/PI staining

XFM and SCM cells (5×10^3 cells/cm^2) were seeded into 12-multiwell plates and cultured for 14 days. The cultured cells were collected using trypsin-EDTA on day 6, when they were considered to be in the logarithmic growth phase, and on day 14, in the over-confluent phase. Apoptotic cells were flow-cytometrically determined using the Annexin V/PI system, as described. The results were expressed as the ratio of the number of the apoptotic cells on day 14 to that on day 6.

Bromodeoxyuridine (BrdU) staining

Cell-proliferative potential was monitored by BrdU staining. Both types of cells were seeded at 5×10^3 cells/cm^2 in 4-well chamber slides (Thermo Fisher Scientific). On days 6 and 14 post-seeding, 10 μM BrdU (Merck KGaA) was added to the cultures, which were then incubated for 3 hours at 37°C prior to fixation. BrdU incorporation was determined with mouse monoclonal anti-BrdU primary antibody (diluted 1:200; Roche Diagnostics) and Alexa 488-conjugated goat polyclonal anti-mouse IgG secondary antibody (diluted 1:1000; Life Technologies, Carlsbad, CA, USA). BrdU-positive cells were counted in 10 random fields under a confocal laser-scanning microscope (LSM 700; Carl Zeiss).

Senescence-associated β-galactosidase (SA β-gal) staining

To examine SA β-gal activity, cultured cells were stained using a senescence cells histochemical staining kit (Merck KGaA) according to manufacturer instructions. Briefly, over-confluent cultures on day 14 were subcultured in 60-mm culture dishes. The cell aggregates after SA β-gal staining were examined using a Biorevo BZ-9000 microscope (Keyence).

Periodic acid-Schiff (PAS) staining

To identify lipofuscin granules, cultured cells were stained by PAS staining, as previously reported [30]. Briefly, cell aggregates derived from subcultured over-confluent cells were fixed in 4% PFA, embedded in paraffin, and sectioned at 5-μm thickness. Deparaffinized sections were subjected to PAS staining, and images were obtained using an Axio imager M2 microscope (Carl Zeiss).

Statistical analysis

Statistical analyses were performed using IBM SPSS statistics software (version 23.0; IBM Japan, Tokyo, Japan). All experiments were independently repeated in triplicate, and values were expressed as the mean ± standard deviation (SD). For two-group comparisons, an unpaired *t* test or a Mann–Whitney *U* test for nonparametric data was used. The chi-square test was used to compare the presence of BrdU-positive cells. For all statistical analyses, *P*-values of < 0.01 indicated a statistically significant difference.

Results

Primary culture and morphological observation of XFM cells

Dental pulp cells enzymatically isolated from the dental pulp tissue of extracted teeth that had been transported in FBS-free basic culture medium were cultured in FBS-free culture medium (XFM) as a primary culture. Notably, the duration required to show cell division of adhered cells in primary cultured XFM cells was significantly longer than that required to form a so-called cell colony from primary culture of SCM cells on fibronectin-precoated culture dishes (9.0 ± 1.8 vs. 6.0 ± 1.7 days; $n = 6$; $P = 0.012$) and on non-coated culture dishes (12.0 ± 1.9 vs. 6.0 ± 1.9 days; $n = 6$; $P = 0.001$). After showing stable cell growth in primary culture, XFM cells showed active proliferation and appeared to form a multitude of small foci of accumulated cells surrounded by many solitary cells, whereas SCM cells formed cell colonies that were likely derived from single cells (Fig. 1a). Following conventional subculture, subconfluent XFM and SCM cells exhibited a fibroblast-like morphology (Fig. 1a). Notably, XFM cells showed thin, spindle-shaped morphology with longer cell processes, regardless of the use of non-fibronectin-precoated dishes (Additional file 1: Fig. S1) as compared with SCM cells. Quantitatively, the adhesive area of XFM cells was significantly smaller than that of SCM cells ($P < 0.01$; Fig. 1b). However, flow-cytometric analysis indicated similar single-cell sizes in XFM and SCM cell suspensions (Fig. 1c).

Upon reaching confluence on day 10 post-seeding, XFM and SCM cells showed similar confluent monolayers according to phase-contrast and fluorescence-microscope observation (Fig. 1d). Intriguingly, when both cultures reached over-confluence on day 14, XFM cells exhibited a thicker, multilayered appearance than did SCM cells (Fig. 1d).

To visualize the fine structure of over-confluent cell cultures, 3D fluorescence-image analysis was conducted using a confocal laser-scanning microscope. 3D imaging revealed that Phalloidin-labeled XFM cells formed extensive, thick multilayers, whereas SCM cells maintained a monolayer structure (Fig. 1e and Additional file 2: Movie S1). HE staining confirmed the multilayered and monolayered structures formed by XFM and SCM cells, respectively (Fig. 1e). Notably, over-confluent SCM cells cultured on fibronectin-precoated culture dishes formed a monolayered structure (Additional file 3: Fig. S2). To confirm whether XFM cells with multilayered appearances on day 14 caused neoplastic transformation, ECLIA was performed using the conditioned media collected from both types of cells. As a result, we detected no common neoplastic/tumorigenic markers (CEA, SCC, or NSE) in either cell culture.

In vitro and *in vivo* stem cell characterization of XFM cells

We previously established a unique *in vitro* cytotoxic susceptibility test of cultured cells under serum-free culture conditions, in addition to characterizing common MSC properties [28]. First, we demonstrated *in vitro* stem cell properties of XFM and SCM cells, including active cell growth (Fig. 2a), a normal karyotype (Fig. 2b), global gene/protein expression associated with the MSC phenotype (Fig. 2c and d), and trilineage differentiation potential, such as osteogenic, adipogenic, and chondrogenic lineages (Fig. 2e–g). Notably, the PDT of XFM cells was 20.1 ± 2.7 h (n = 3), which was markedly shorter than that of SCM cells (28.5 ± 3.7 h; n = 3). Collectively, these data indicated that XFM cells possessed high proliferative ability and typical MSC characteristics along with chromosomal stability.

Second, we assessed the cellular susceptibility of XFM and SCM cells to cytotoxic stimuli. As a positive control for cell damage, staurosporine affected both types

of cells to the same degree, as expected. After H_2O_2 and UV radiation, both cell types showed degenerative changes in cell morphology (Fig. 3a). Flow cytometry with Annexin V/PI staining quantitatively indicated that the damaged cells cultured in XFM were significantly higher in number than those cultured in SCM after H_2O_2 and UV treatments ($P < 0.01$; Fig. 3b and c).

Finally, we performed an *in vivo* transplantation experiment using *ex vivo*-expanded DPSCs cultured in XFM and SCM. HE and MT staining indicated that both types of cell/HA constructs that were subcutaneously transplanted showed osteo-dentin hard-tissue formation 16 weeks after transplantation, whereas the HA constructs alone (without cells) did not form such hard tissue (Fig. 4). Tumor formation was not observed in any of the samples. Immunohistochemistry demonstrated that the cells within newly formed hard tissue stained intensely with anti-vimentin and -DSP antibodies in both cell/HA constructs, whereas no positive immunoreactivity was observed in the HA constructs (Fig. 4). The immunoreactivity of the vimentin antibody was mainly observed in mesenchymal stromal cells within native dental pulp and alveolar bone, whereas DSP was preferentially observed in odontoblasts in the dental pulp, but not in osteocytes within the alveolar bone (Additional file 4: Fig. S3).

Over-confluent XFM cells show disrupted proliferative behavior

From the growth curves presented in Fig. 2a, we found that the number of XFM cells declined as of day 14 when the cultures reached the over-confluent state (Fig. 1e). By contrast, SCM cell growth showed a sustained plateau at this time point. Moreover, we microscopically observed a considerable number of cells with a condensed nucleus within the multilayered XFM cells, but not within the SCM monolayers (Fig. 1d and e). To clarify the reason for the reduced number of cells and nuclear condensation in the XFM

culture, we conducted a TUNEL assay using over-confluent cultures on day 14. Notably, over-confluent multilayered XFM cells contained a substantial amount of TUNEL-positive cells, whereas monolayered SCM cells were completely TUNEL-negative (Fig. 5a). Flow-cytometric analysis using Annexin V/PI staining quantitatively indicated that the apoptotic cells in XFM culture were significantly higher in number than those in SCM culture ($P < 0.01$; Fig. 5b and c).

To examine whether cell division occurred, BrdU-incorporation analysis was used. We first determined the BrdU-uptake level of cultured cells on day 6 when they reached the logarithmic growth phase. As expected, both types of cells showed nearly the same level of BrdU incorporation (N.S.; Fig. 5d and e). Surprisingly, in over-confluent XFM cells, the level of BrdU uptake on day 14 was comparable to that on day 6, whereas it was significantly decreased in SCM cells at this time point ($P < 0.01$; Fig. 5d and e). Notably, a large number of BrdU-positive cells within the multilayered XFM cells had a condensed nucleus (Additional file 5: Fig. S4).

Finally, we explored time-course gene-expression profiles of apoptosis- and cell cycle-related markers during cell growth by RT-PCR. Although both types of cells expressed the pro-apoptotic gene *Bax* at a similar level, the anti-apoptotic gene *Bcl-2* was downregulated in XFM cells as the culture progressed, whereas it maintained a steady expression level in SCM cells (Fig. 5f; Additional file 6: Fig. S5). The cell cycle inhibitors *p21*, *p16*, and *p53* were expressed at lower levels in XFM as compared with those in SCM cells throughout the culture (Fig. 5f; Additional file 6: Fig. S5). On day 14, *p53* was upregulated in XFM cells, which at this time point showed the multilayered structure containing extensive TUNEL-positive cells. Briefly, the reduction in the number of XFM cells on day 14 was caused by apoptotic cell death, whereas the proliferative potential in the over-confluent XFM cultures was maintained at the level seen in the logarithmic

growth phase.

Aberrant proliferative behavior of over-confluent XFM cells negatively affects subculture

Next, we subcultured both types of over-confluent cultures on day 14 using a conventional trypsin/EDTA procedure. Surprisingly, XFM cells predominantly formed cell aggregates and did not proliferate further, whereas SCM cells were normally passaged and reached confluence (Fig. 6). The XFM-cell aggregates were entirely positive for the cellular senescence marker SA β-gal. Moreover, HE staining indicated that the cell aggregates accumulated apoptotic cells with condensed nuclei, and the senescent cells contained perinuclear lipofuscin granules exhibiting autofluorescence. To confirm these findings, specific histochemical staining for apoptosis or lipofuscin granules was performed. TUNEL-positive/condensed nuclei and PAS-positive small granules were clearly observed within the XFM-cell aggregates (Fig. 6).

Cryopreservation does not affect the stem cell characteristics and cellular behaviors of XFM cells

We obtained comparable results for all of the aforementioned experiments using cryopreserved XFM cells (Additional files 7–12: Figs. S6–S11).

Discussion

Reliable *ex vivo* isolation and expansion of donor-derived MSCs are required for establishing practical cell therapies. The supplementation of culture media with xenogeneic serum, including FBS, is widely accepted and believed to be essential for facilitating primary cell adhesion and subsequent cell growth in MSC culture. Although several FBS-free culture media have been developed and are widely used for the expansion of subcultured MSCs after passaging [31–33], no studies have investigated whether the FBS-free culture condition is suitable for isolation and primary culture of MSCs derived from dental pulp tissue, except for one study that reported its usability for primary isolation of a neurogenic cell population from dental pulp [34].

In this study, we examined whether the MSC population can be isolated from dental pulp tissue using cell isolation involving FBS-free basic medium for transporting extracted teeth, and whether a commercially available FBS-free culture medium is suitable for primary culture and further expansion of DPSCs. The results showed that the significantly thinner and spindle-shaped XFM cells could be isolated in primary culture and then routinely subcultured. Interestingly, although primary cultured XFM cells took a significantly longer time to adhere to the culture dishes than did SCM cells, subcultured XFM cells showed significantly greater proliferation than did SCM cells. Moreover, *ex vivo*-expanded XFM cells exhibited typical MSC characteristics, including marker gene/protein expression, trilineage differentiation potential, and hard, osteo-dentin tissue formation. Additionally, long-term-cultured XFM cells maintained a normal karyotype *in vitro* and non-tumorigenic potential *in vivo*. These results suggested that DPSCs can be reliably and safely isolated and expanded *in vitro* under FBS-free culture conditions.

However, this study revealed multiple safety concerns when handling DPSCs under FBS-free culture conditions. First, XFM cells were more susceptible to damage, as determined using the extrinsic cytotoxic stimuli H_2O_2 and UV light, suggesting that culture medium without FBS does not protect cultured DPSCs against extrinsic cytotoxicity, which is consistent with the previously reported cytotoxic susceptibility of periodontal ligament-derived MSCs [28]. Second, excessive cultivation (i.e., over-confluency of XFM cells) should be avoided, as this resulted in a reduction of the number of XFM cells that can be obtained at one time and the disruption of the proliferative behavior of XFM cells that form a multilayered structure consisting of both considerable TUNEL-positive apoptotic cells and BrdU-positive proliferating cells. Intriguingly, this aberrant proliferative behavior affected subcultured XFM cells after passaging at the over-confluent state. Thirdly, subcultured over-confluent XFM cells predominantly formed cell aggregates consisting of replicatively senescent and apoptotic cells and are indeed difficult to expand further.

The aberrant cell-proliferative behaviors appeared attributable to the substantial amounts of both TUNEL-positive and BrdU-positive cells. The apoptotic cells were confirmed by time-course gene-expression patterns as determined by RT-PCR, which revealed downregulation of anti-apoptotic *Bcl-2* and upregulation of the p53-dependent apoptotic pathway [35]. Cell cycle progression in proliferating cells depends upon the downregulation of *p21* and *p16*, which are closely related to cell cycle arrest [36]. Moreover, we frequently observed BrdU-positive cells with condensed nuclei within the multilayered XFM cultures. In general, BrdU is used to detect cells entering the S phase of the cell cycle; however, a recent study described that replicatively senescent cells are arrested in not only G1 but also G2 phase, which follows the S phase [37]. Therefore, the BrdU-positive/condensed-nucleus cells were considered to be G2-arrested senescent cells.

Intriguingly, we also observed that XFM cells formed considerable accumulations in primary culture and showed active proliferation and formed overlapping layers in subcultures. By contrast, SCM cells did not form accumulations during primary cultivation or multiple layers exhibiting excessive cell death/division after reaching confluence, regardless of the use of fibronectin-precoated culture dishes, suggesting that the contribution of extracellular matrix (ECM) is not responsible for the formation of cellular accumulation and multilayers. A possible mechanism of these unique proliferative behaviors is that XFM cells lose or exhibit attenuated "contact inhibition" dependent upon cell–cell interactions, although an alternative possibility is that cellular adhesion to ECM components still remains. Therefore, although further studies are needed to clarify the possible signaling pathways involved in both the contact inhibition and cellular behaviors, the presence of xenogeneic serum components likely contributes to contact inhibition and controls cell behavior, as evident from the monolayered growth of SCM cells throughout the cell culture.

Ex vivo-expanded DPSCs are routinely cryopreserved in cell banks until use for cell therapy in the clinic. Furthermore, a simple and reliable procedure is desired for the manipulation and therapeutic preparation of DPSCs. Hence, we independently conducted the aforementioned *in vitro* and *in vivo* experiments using DMSO-free cryopreserved XFM-cell stocks. The results indicated that thawed XFM cells showed comparable stem cell characteristics and aberrant proliferative behaviors to those of non-cryopreserved XFM cells. Therefore, cryopreservation of XFM cells would be very useful for research and clinical use. Consequently, the findings of this comprehensive study hold promise for optimal practical cell-culture protocols for handling DPSCs under xenogeneic serum-free culture conditions.

Conclusion

This report described the first successful isolation and expansion of an MSC population from donor-derived tissue (dental pulp) under xenogeneic serum-free culture conditions and demonstrated the suitability of serum-free culture medium for application in DMSO-free cryopreservation. Although xenogeneic serum-free cultivation facilitates effective large-scale expansion of DPSCs, excessive cultivation to over-confluence should be avoided, because this abrogates the proliferative potential and further cultivation of XFM cells. Establishing appropriate xenogeneic serum-free culture conditions in future studies will enable us to obtain clinically feasible MSCs from dental pulp tissue, which represents a readily accessible cell source for stem cell research & therapy.

List of abbreviations

MSC: Mesenchymal stem cell; DPSC: Dental pulp stem cell; FBS: fetal bovine serum; XFM: Xenogeneic serum-free culture medium; SCM: Xenogeneic serum-containing culture medium; EDTA: Ethylenediaminetetraacetic acid; DMSO: Dimethyl sulfoxide; PFA: Paraformaldehyde; PBS: Calcium- and magnesium-free phosphate-buffered saline; DAPI: 4′,6-diamidino-2-phenylindole; 3D: Three-dimensional; PDT: Population doubling time; Ig: Immunoglobulin; RT-PCR: Reverse-transcription polymerase chain reaction; H_2O_2: hydrogen peroxide; UV: Ultraviolet; PI: Propidium iodide; HA: Hydroxyapatite/β-tricalciumphosphate; HE: Hematoxylin and eosin; MT: Masson's trichrome; DSP: Dentin sialoprotein; TUNEL: Terminal deoxynucleotidyl transferase-mediated deoxyuridine triphosphate nick-end labeling; BrdU: Bromodeoxyuridine; SA β-gal: Senescence-associated β-galactosidase; PAS: Periodic acid-Schiff; SD: Standard deviation.

Declarations

Acknowledgements

The author would like to express the deepest appreciation to Prof. Taka Nakahara for his sustained supervision, critical reviewing of the thesis, and fruitful discussions. The author also thanks Drs. Tetsuro Horie and Kazutoshi Sato for providing scientific advice. This study is based on a thesis submitted by Mai Mochizuki to Graduate School of Life Dentistry at Tokyo, The Nippon Dental University, in partial fulfillment of the requirements for the degree of Doctor of Philosophy.

Funding

This work was supported by a Grant-in-Aid for Young Scientists (A) (No. 24689073) and a Grant-in-Aid for Scientific Research (B) (No. 15H05046) from the Japan Society for the Promotion of Science (JSPS KAKENHI), and it was supported in part by a Research Grant (2015) from the Nippon Dental University.

Availability of data and materials

All data generated or analyzed during this study are included in this published article and its supplementary information files.

Competing interests

The author declares that they have no competing interests.

Consent for publication

Not applicable.

Ethics approval and consent to participate

The present study was approved by the ethics committee of Nippon Dental University School of Life Dentistry at Tokyo (Approval No. NDU-T2013-10) and it was conducted in accordance with the amended Declaration of Helsinki. Informed consent was obtained from all individual donors after fully explaining the nature of the procedure and the intended use of the tissue obtained. All animal experiments were performed in accordance with the “Regulations for Animal Experimentation and Laboratory Animal Facility” in the Nippon Dental University School of Life Dentistry at Tokyo. The procedure was approved by the Animal Experiments Committee of the Nippon Dental University School of Life Dentistry at Tokyo.

References

1. Burger SR. Current regulatory issues in cell and tissue therapy. Cytotherapy. 2003;5:289-98.
2. Kordelas L, Rebmann V, Ludwig AK, Radtke S, Ruesing J, Doeppner TR, Epple M, Horn PA, Beelen DW, Giebel B. MSC-derived exosomes: a novel tool to treat therapy-refractory graft-versus-host disease. Leukemia. 2014;28:970-3.
3. He A, Liu L, Luo X, Liu Y, Liu Y, Liu F, Wang X, Zhang Z, Zhang W, Liu W, Cao Y, Zhou G. Repair of osteochondral defects with in vitro engineered cartilage based on autologous bonemarrow stromal cells in a swine model. Sci Rep. 2017;7:40489.
4. Golpanian S, Wolf A, Hatzistergos KE, Hare JM. Rebuilding the damaged heart: mesenchymal stem cells, cell-based therapy, and engineered heart tissue. Physiol Rev. 2016;96:1127-68.
5. Caminal M, Peris D, Fonseca C, Barrachina J, Codina D, Rabanal RM, Moll X, Morist A, García F, Cairó JJ, Gòdia F, Pla A, Vives J. Cartilage resurfacing potential of PLGA scaffolds loaded with autologous cells from cartilage, fat, and bone marrow in an ovine model of osteochondral focal defect. Cytotechnology. 2016;68:907-19.
6. Wang Y, Han ZB, Song YP, Han ZC. Safety of mesenchymal stem cells for clinical application. Stem Cells Int. 2012; doi: 10.1155/2012/652034.
7. Chase LG, Lakshmipathy U, Solchaga LA, Rao MS, Vemuri MC. A novel serum-free medium for the expansion of human mesenchymal stem cells. Stem Cell Res Ther. 2010;1:8.
8. Tamaki Y, Nakahara T, Ishikawa H, Sato S. In vitro analysis of mesenchymal stem cells derived from human teeth and bone marrow. Odontology. 2013;101:121-32.

9. Odontology prize 2017. Odontology. 2017;105:391. doi: 10.1007/s10266-017-0325-2.
10. Gronthos S, Mankani M, Brahim J, Robey PG, Shi S. Postnatal human dental pulp stem cells (DPSCs) in vitro and in vivo. Proc Natl Acad Sci USA. 2000;97:13625-30.
11. Nuti N, Corallo C, Chan BM, Ferrari M, Gerami-Naini B. Multipotent differentiation of human dental pulp stem cells: a literature review. Stem Cell Rev. 2016;12:511-523.
12. Martens W, Sanen K, Georgiou M, Struys T, Bronckaers A, Ameloot M, Phillips J, Lambrichts I. Human dental pulp stem cells can differentiate into Schwann cells and promote and guide neurite outgrowth in an aligned tissue-engineered collagen construct in vitro. FASEB J. 2014;28:1634-43.
13. Karaöz E, Demircan PC, Sağlam O, Aksoy A, Kaymaz F, Duruksu G. Human dental pulp stem cells demonstrate better neural and epithelial stem cell properties than bone marrow-derived mesenchymal stem cells. Histochem Cell Biol. 2011;136:455-73.
14. Armiñán A, Gandía C, Bartual M, García-Verdugo JM, Lledó E, Mirabet V, Llop M, Barea J, Montero JA, Sepúlveda P. Cardiac differentiation is driven by NKX2.5 and GATA4 nuclear translocation in tissue-specific mesenchymal stem cells. Stem Cells Dev. 2009;18:907-18.
15. Ishkitiev N, Yaegaki K, Calenic B, Nakahara T, Ishikawa H, Mitiev V, Haapasalo M. Deciduous and permanent dental pulp mesenchymal cells acquire hepatic morphologic and functional features in vitro. J Endod. 2010;36:469-74.
16. Ishkitiev N, Yaegaki K, Imai T, Tanaka T, Fushimi N, Mitev V, Okada M, Tominaga N, Ono S, Ishikawa H. Novel management of acute or secondary biliary liver conditions using hepatically differentiated human dental pulp cells. Tissue Eng Part A. 2015;21:586-93.

17. d'Aquino R, Graziano A, Sampaolesi M, Laino G, Pirozzi G, De Rosa A, Papaccio G. Human postnatal dental pulp cells co-differentiate into osteoblasts and endotheliocytes: a pivotal synergy leading to adult bone tissue formation. Cell Death Differ. 2007;14:1162-71.
18. Zhang J, Lu X, Feng G, Gu Z, Sun Y, Bao G, Xu G, Lu Y, Chen J, Xu L, Feng X, Cui Z. Chitosan scaffolds induce human dental pulp stem cells to neural differentiation: potential roles for spinal cord injury therapy. Cell Tissue Res. 2016;366:129-42.
19. Gandia C, Armiñan A, García-Verdugo JM, Lledó E, Ruiz A, Miñana MD, Sanchez-Torrijos J, Payá R, Mirabet V, Carbonell-Uberos F, Llop M, Montero JA, Sepúlveda P. Human dental pulp stem cells improve left ventricular function, induce angiogenesis, and reduce infarct size in rats with acute myocardial infarction. Stem Cells. 2008;26:638-45.
20. d'Aquino R, De Rosa A, Lanza V, Tirino V, Laino L, Graziano A, Desiderio V, Laino G, Papaccio G. Human mandible bone defect repair by the grafting of dental pulp stem/progenitor cells and collagen sponge biocomplexes. Eur Cell Mater. 2009;18:75-83.
21. Nakashima M, Iohara K, Murakami M, Nakamura H, Sato Y, Ariji Y, Matsushita K. Pulp regeneration by transplantation of dental pulp stem cells in pulpitis: a pilot clinical study. Stem Cell Res Ther. 2017;8:61.
22. Gregory CA, Reyes E, Whitney MJ, Spees JL. Enhanced engraftment of mesenchymal stem cells in a cutaneous wound model by culture in allogenic species-specific serum and administration in fibrin constructs. Stem Cells. 2006;24:2232-43.

23. Spees JL, Gregory CA, Singh H, Tucker HA, Peister A, Lynch PJ, Hsu SC, Smith J, Prockop DJ. Internalized antigens must be removed to prepare hypoimmunogenic mesenchymal stem cells for cell and gene therapy. Mol Ther. 2004;9:747-56.
24. Sato K, Itoh T, Kato T, Kitamura Y, Kaul SC, Wadhwa R, Sato F, Ohneda O. Serum-free isolation and culture system to enhance the proliferation and bone regeneration of adipose tissue-derived mesenchymal stem cells. In Vitro Cell Dev Biol Anim. 2015;51:515-29.
25. Ishkitiev N, Yaegaki K, Imai T, Tanaka T, Nakahara T, Ishikawa H, Mitev V, Haapasalo M. High-purity hepatic lineage differentiated from dental pulp stem cells in serum-free medium. J Endod. 2012;38:475-80.
26. Wang Y, Wu H, Yang Z, Chi Y, Meng L, Mao A, Yan S, Hu S, Zhang J, Zhang Y, Yu W, Ma Y, Li T, Cheng Y, Wang Y, Wang S, Liu J, Han J, Li C, Liu L, Xu J, Han ZB, Han ZC. Human mesenchymal stem cells possess different biological characteristics but do not change their therapeutic potential when cultured in serum free medium. Stem Cell Res Ther. 2014;5:132.
27. Shinagawa-Ohama R, Mochizuki M, Tamaki Y, Suda N, Nakahara T. Heterogeneous human periodontal ligament-committed progenitor and stem cell populations exhibit a unique cementogenic property under in vitro and in vivo conditions. Stem Cells Dev. 2017;26:632-45.
28. Murabayashi D, Mochizuki M, Tamaki Y, Nakahara T. Practical methods for handling human periodontal ligament stem cells in serum-free and serum-containing culture conditions under hypoxia: implications for regenerative medicine. Hum Cell. 2017;30:169-80.

29. Tominaga N, Nakahara T, Nasu M, Satoh T. Isolation and characterization of epithelial and myogenic cells by "fishing" for the morphologically distinct cell types in rat primary periodontal ligament cultures. Differentiation. 2013;85:91-100.
30. Nakahara T, Tominaga N, Toyomura J, Tachibana T, Ide Y, Ishikawa H. Isolation and characterization of embryonic ameloblast lineage cells derived from tooth buds of fetal miniature swine. In Vitro Cell Dev Biol Anim. 2016;52:445-53.
31. Bonnamain V, Thinard R, Sergent-Tanguy S, Huet P, Bienvenu G, Naveilhan P, Farges JC, Alliot-Licht B. Human dental pulp stem cells cultured in serum-free supplemented medium. Front Physiol. 2013;4:357.
32. Riordan NH, Madrigal M, Reneau J, de Cupeiro K, Jiménez N, Ruiz S, Sanchez N, Ichim TE, Silva F, Patel AN. Scalable efficient expansion of mesenchymal stem cells in xeno free media using commercially available reagents. J Transl Med. 2015;13:232.
33. Hirata TM, Ishkitiev N, Yaegaki K, Calenic B, Ishikawa H, Nakahara T, Mitev V, Tanaka T, Haapasalo M. Expression of multiple stem cell markers in dental pulp cells cultured in serum-free media. J Endod. 2010;36:1139-44.
34. Jung J, Kim JW, Moon HJ, Hong JY, Hyun JK. Characterization of neurogenic potential of dental pulp stem cells cultured in xeno/serum-free condition: in vitro and in vivo assessment. Stem Cells Int. 2016; doi: 10.1155/2016/6921097.
35. Miyashita T, Reed JC. Tumor suppressor p53 is a direct transcriptional activator of the human bax gene. Cell. 1995;80:293-9.
36. Serrano M, Hannon GJ, Beach D. A new regulatory motif in cell-cycle control causing specific inhibition of cyclin D/CDK4. Nature. 1993;366:704-7.
37. Mao Z, Ke Z, Gorbunova V, Seluanov A. Replicatively senescent cells are arrested in G1 and G2 phases. Aging (Albany NY). 2012;4:431-5.

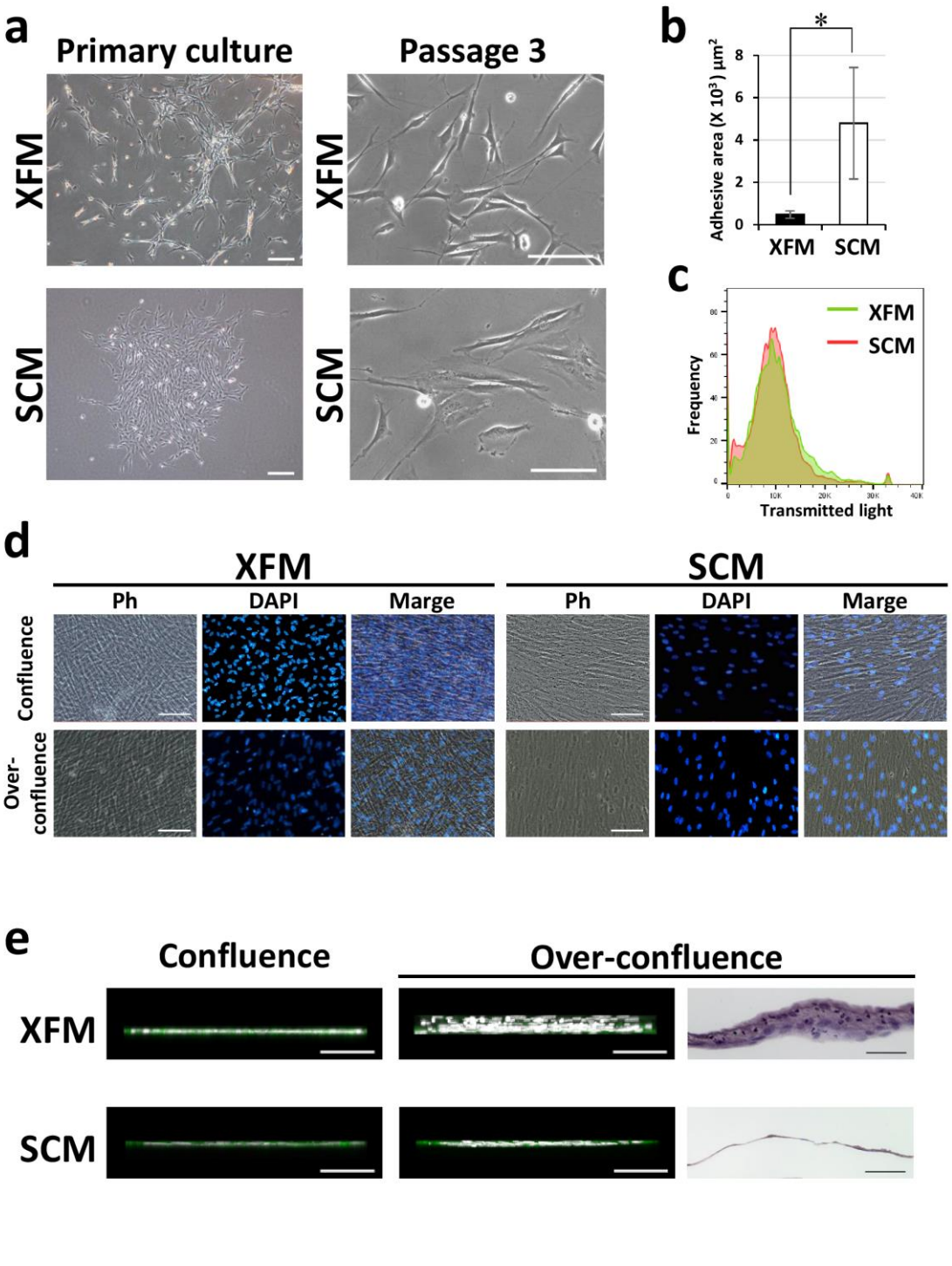
a
Primary culture
Passage 3
XFM
XFM
SCM
SCM
b
*
Adhesive area (X 10³) µm²
8
6
4
2
0
XFM
SCM
c
XFM
SCM
Frequency
Transmitted light
d
XFM
SCM
Ph
DAPI
Marge
Ph
DAPI
Marge
Confluence
Over-confluence
e
Confluence
Over-confluence
XFM
SCM

Fig. 1

Morphological appearance and morphometric analysis of DPSCs under xenogeneic serum-free or FBS-containing culture conditions. **a** Phase-contrast images of DPSCs cultured in XFM or SCM in primary culture. Scale bars, 200 μm. Passage 3: scale bars, 100 μm. **b** Cell morphometric evaluation of adhesive areas of XFM and SCM cells at passage 3. *$P < 0.01$. **c** Flow-cytometric analysis of single-cell size in XFM and SCM cellular suspensions. **d** Phase-contrast and fluorescence-microscope images of DAPI-labeled XFM and SCM cells at confluence on day 10 or over-confluence on day 14 post-seeding. Scale bars, 100 μm. **e** 3D fluorescence imaging and HE staining of confluent and over-confluent cultures of Phalloidin-labeled XFM and SCM cells. Scale bars, 100 μm.

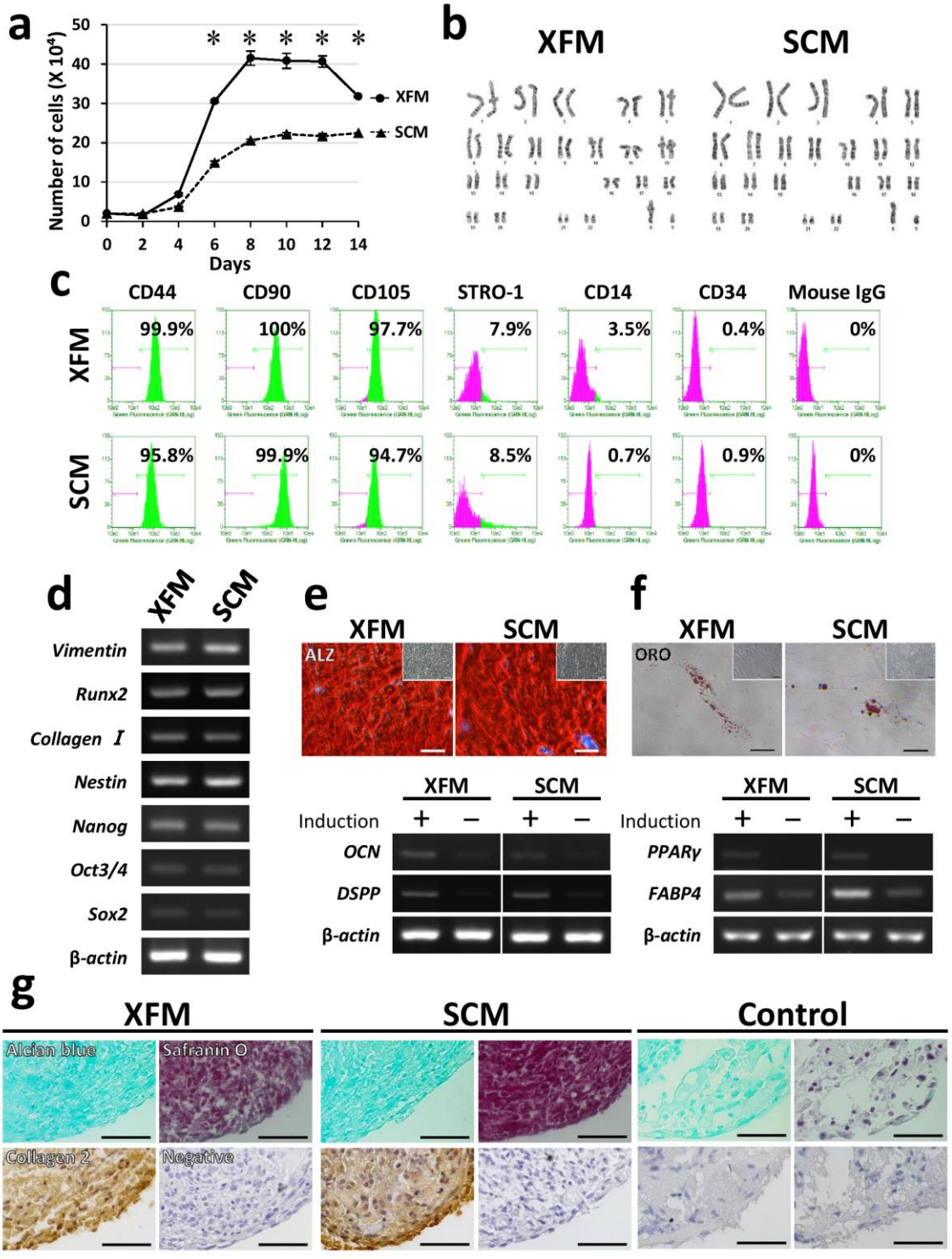
a
Number of cells (X 10⁴)
Days
XFM
SCM
b
XFM
SCM
c
CD44
CD90
CD105
STRO-1
CD14
CD34
Mouse IgG
99.9%
100%
97.7%
7.9%
3.5%
0.4%
0%
95.8%
99.9%
94.7%
8.5%
0.7%
0.9%
0%
d
Vimentin
Runx2
Collagen I
Nestin
Nanog
Oct3/4
Sox2
β-actin
e
ALZ
Induction
OCN
DSPP
β-actin
f
ORO
PPARγ
FABP4
β-actin
g
Alcian blue
Safranin O
Collagen 2
Negative
Control

Fig. 2

Stem cell characterization of DPSCs under xenogeneic serum-free or FBS-containing culture conditions. **a** Growth-curve evaluation of DPSCs cultured in XFM or SCM at passage 3 during 14 days of culture. *$P < 0.01$. **b** Karyotype analysis of XFM and SCM cells at passage 10. **c** Flow cytometry for cell-surface markers of MSCs and hematopoietic cells on XFM and SCM cells. **d** Gene-expression profile of MSC and osteo/odontogenic markers in XFM and SCM cells as determined by RT-PCR. **e** Alizarin red staining (ALZ) and RT-PCR results for osteo/odontogenic marker genes from mineral-inducing cultures of XFM and SCM cells after a 4-week induction (+) or 4 weeks without induction (−). Insets in ALZ images show no-induction cultures (4 weeks). Scale bars, 100 μm. **f** Oil red O-staining (ORO) showing lipid droplets and RT-PCR results for adipogenic marker genes (−) in XFM and SCM cells after a 4-week adipogenic induction (+) or 4 weeks without induction. Insets in ORO images show no-induction cultures (4 weeks). Scale bars, 50 μm. **g** Alcian blue, Safranin O, and immunohistochemical staining showing chondrogenic induction cultures of XFM and SCM cells after 4 weeks. No chondrogenic induction was observed after 4 weeks (control). Scale bars, 50 μm.

Collagen 2, type II collagen.

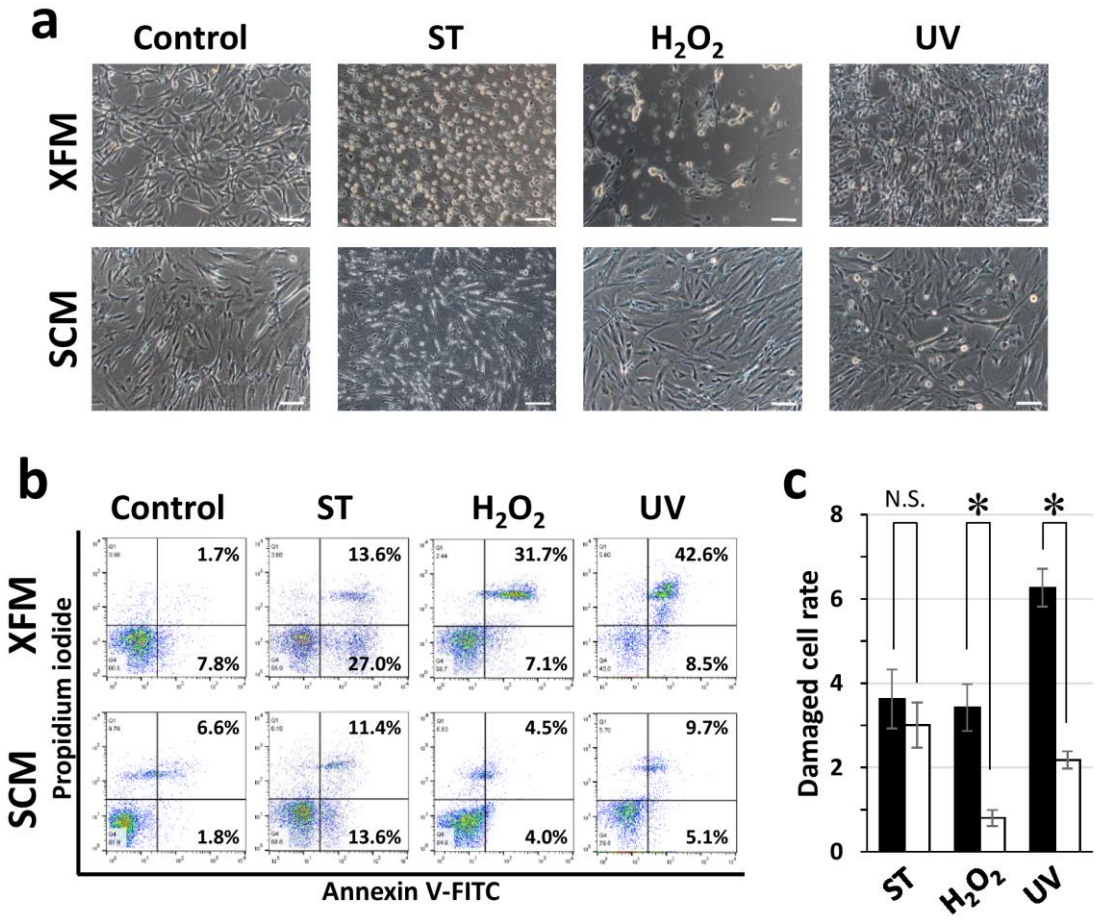

Fig. 3

In vitro assessment of cellular stress/damage of DPSCs induced by extrinsic cytotoxic stimuli under xenogeneic serum-free or FBS-containing culture conditions. **a** Morphological changes of DPSCs cultured in XFM and SCM before (control) and after treatment with staurosporine (ST), H_2O_2, or UV radiation. Scale bars, 100 μm. **b** Flow-cytometric analysis of cytotoxic stimulus-treated XFM and SCM cells using an Annexin V/PI system and **c** quantification of the damaged cells cultured in XFM (black columns) and SCM (white columns). *$P < 0.01$. N.S., no significant difference.

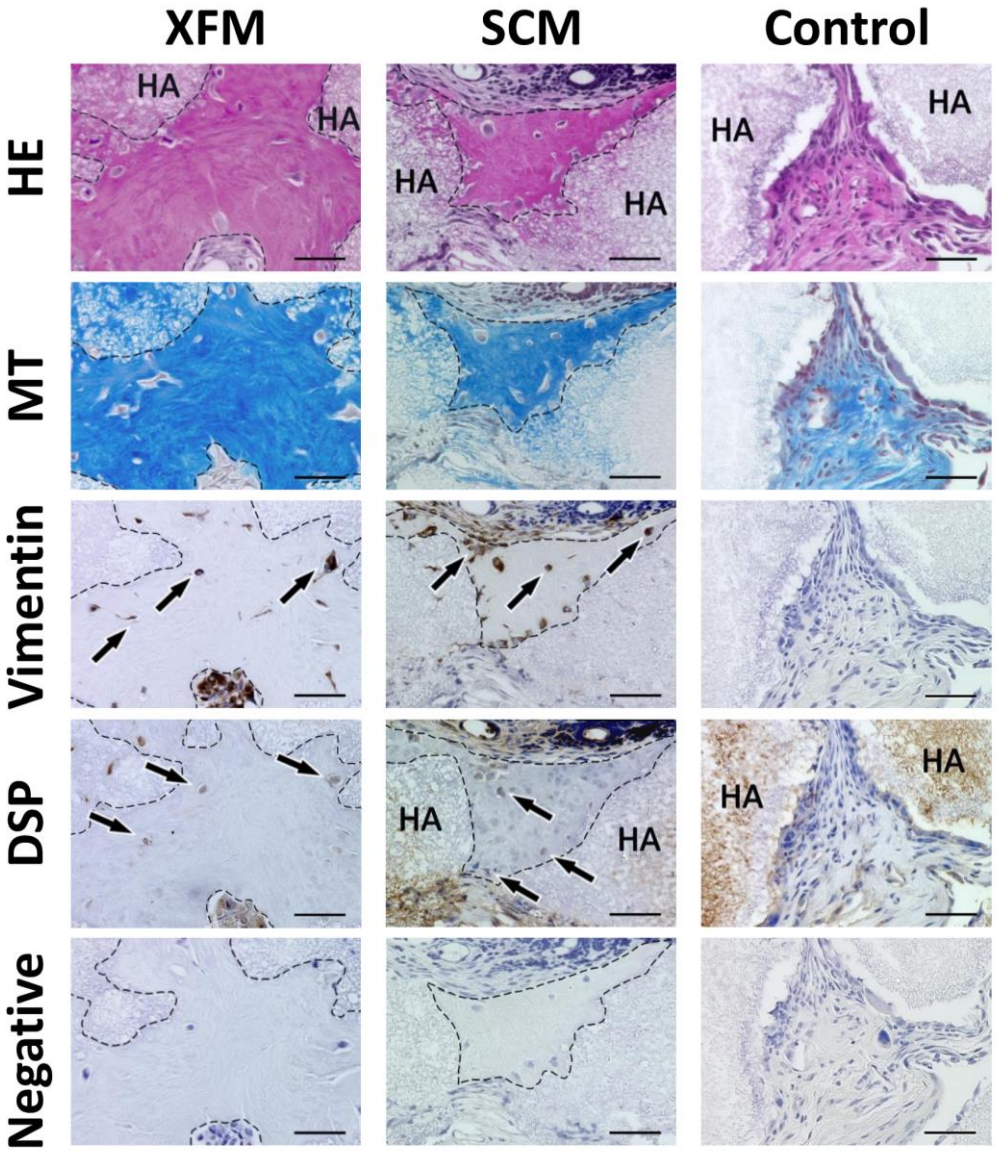

Fig. 4

In vivo subcutaneous transplantation of *ex vivo*-expanded DPSCs cultured in xenogeneic serum-free or FBS-containing culture medium. HA scaffolds containing DPSCs cultured in XFM, SCM, or HA alone (control) were histologically evaluated by HE, MT, and immunohistochemical staining 16 weeks after transplantation. DSP, dentin sialoprotein. Arrows indicate cells embedded within the newly formed hard tissue, which is outlined by dashed lines. The primary antibody was omitted during immunostaining (negative control). Scale bars, 50 μm.

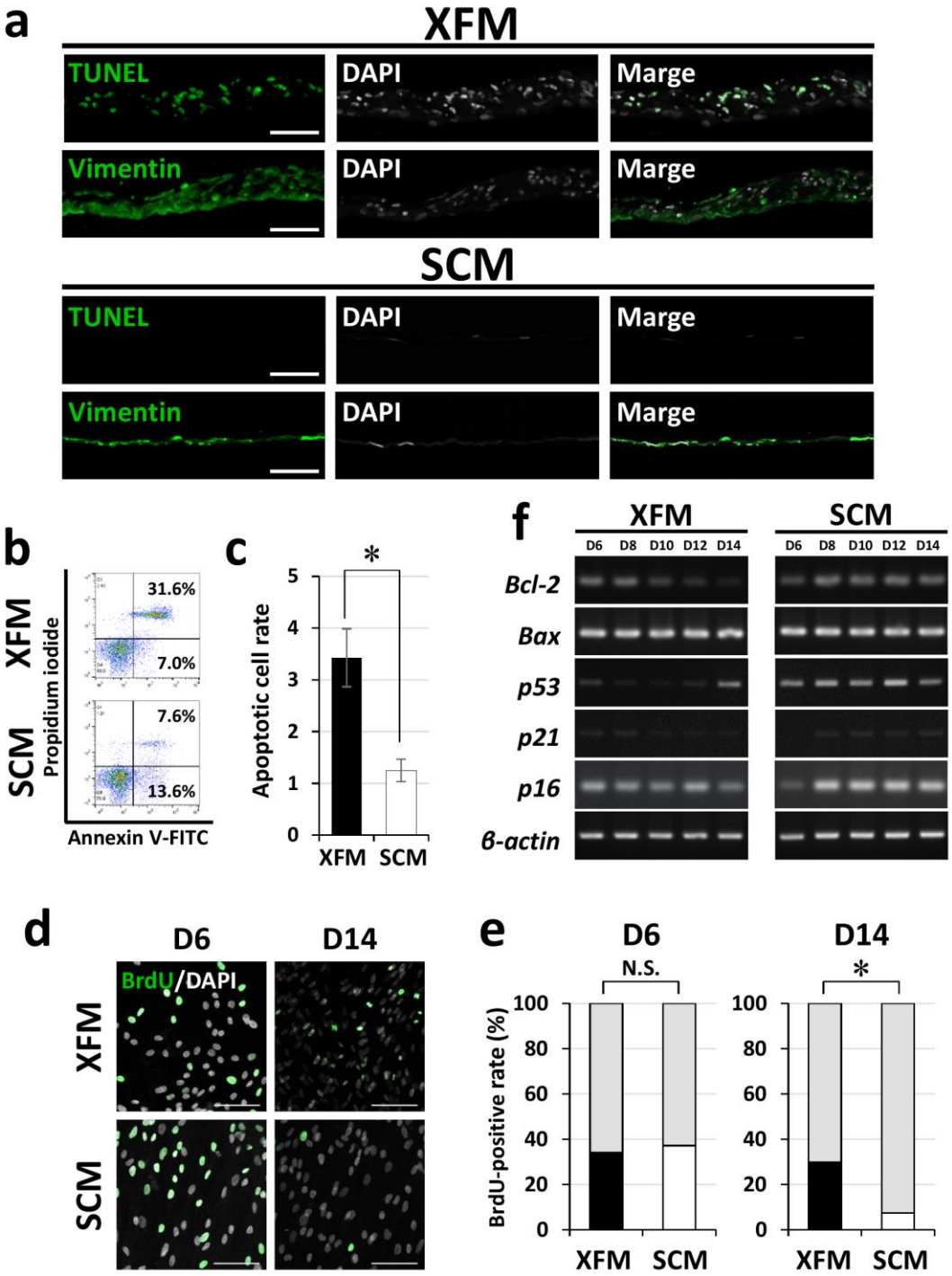
a
XFM
TUNEL
DAPI
Marge
Vimentin
DAPI
Marge
SCM
TUNEL
DAPI
Marge
Vimentin
DAPI
Marge
b
XFM
SCM
Propidium iodide
31.6%
7.0%
7.6%
13.6%
Annexin V-FITC
c
Apoptotic cell rate
*
5
4
3
2
1
0
XFM
SCM
f
XFM
SCM
D6 D8 D10 D12 D14
D6 D8 D10 D12 D14
Bcl-2
Bax
p53
p21
p16
β-actin
d
D6
D14
XFM
SCM
BrdU/DAPI
e
D6
D14
N.S.
*
BrdU-positive rate (%)
100
80
60
40
20
0
XFM
SCM
XFM
SCM

Fig. 5

Cellular behavior of DPSCs at over-confluence under xenogeneic serum-free or FBS-containing culture medium. **a** TUNEL and immunohistochemical staining of over-confluent DPSC cultures in XFM and SCM. Scale bars, 100 μm. **b** Flow-cytometric analysis of over-confluent XFM and SCM cultures using an Annexin V/PI system and **c** quantification of the apoptotic cells $*P < 0.01$. **d** BrdU staining and **e** quantification of BrdU-positive cells in XFM and SCM cultures on day 6 (D6) and day 14 (D14) post-seeding. Scale bars, 100 μm. $*P < 0.01$. **f** Time-course gene-expression profile for apoptosis and cell cycle regulators during cell-growth evaluation of XFM and SCM cells as determined by RT-PCR. N.S., no significant difference.

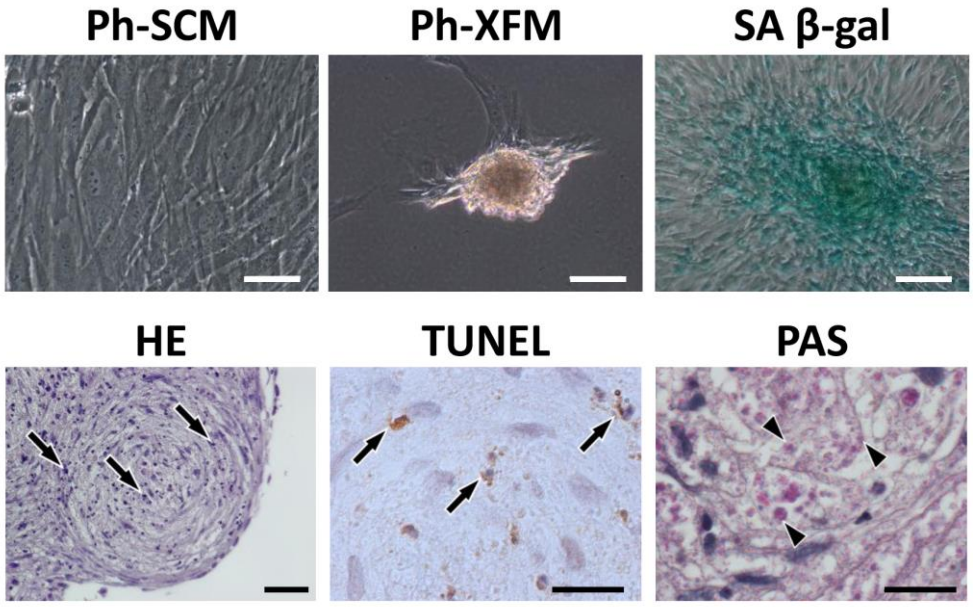

Fig. 6

Cellular-behavioral analysis after subculture of over-confluent DPSCs cultured in xenogeneic serum-free or FBS-containing culture medium. Phase-contrast images of subcultured over-confluent monolayered SCM cells (Ph-SCM) and subcultured over-confluent multilayered XFM cells (Ph-XFM). Scale bars, 50 μm. SA β-gal staining of a cell aggregate derived from subcultured over-confluent XFM cells (SA β-gal). Scale bar, 50 μm. Histological evaluation of a cell aggregate by HE, TUNEL, and PAS staining. Arrows indicate condensed nuclei according to HE staining (scale bar, 50 μm) and TUNEL-positive cells (scale bar, 20 μm). Arrowheads indicate PAS-positive lipofuscin granules. Scale bar, 20 μm.

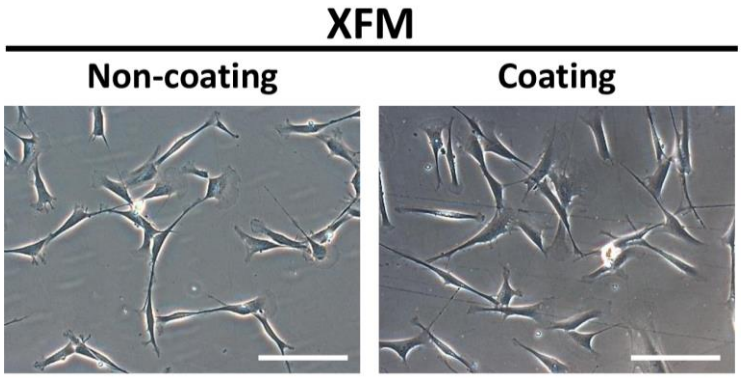

Additional file 1: Fig. S1

Phase-contrast images of DPSCs cultured in xenogeneic serum-free culture medium (XFM) on fibronectin-precoated or non-coated culture dishes. Scale bars, 100 μm.

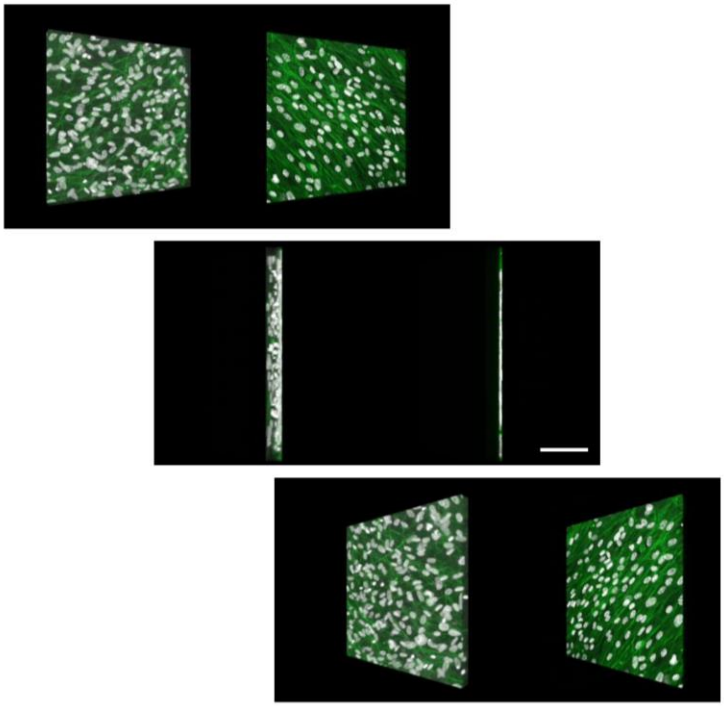

Additional file 2: Movie S1

3D fluorescence image of over-confluent multilayered XFM cells (left) and monolayered SCM cells (right). Scale bar, 100 μm. See https://stemcellres.biomedcentral.com/.

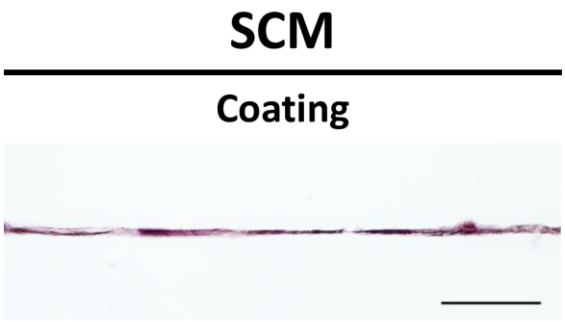

Additional file 3: Fig. S2

HE staining of DPSCs cultured in FBS-containing medium (SCM) on fibronectin-precoated dish after reaching confluence. Scale bar, 100 μm.

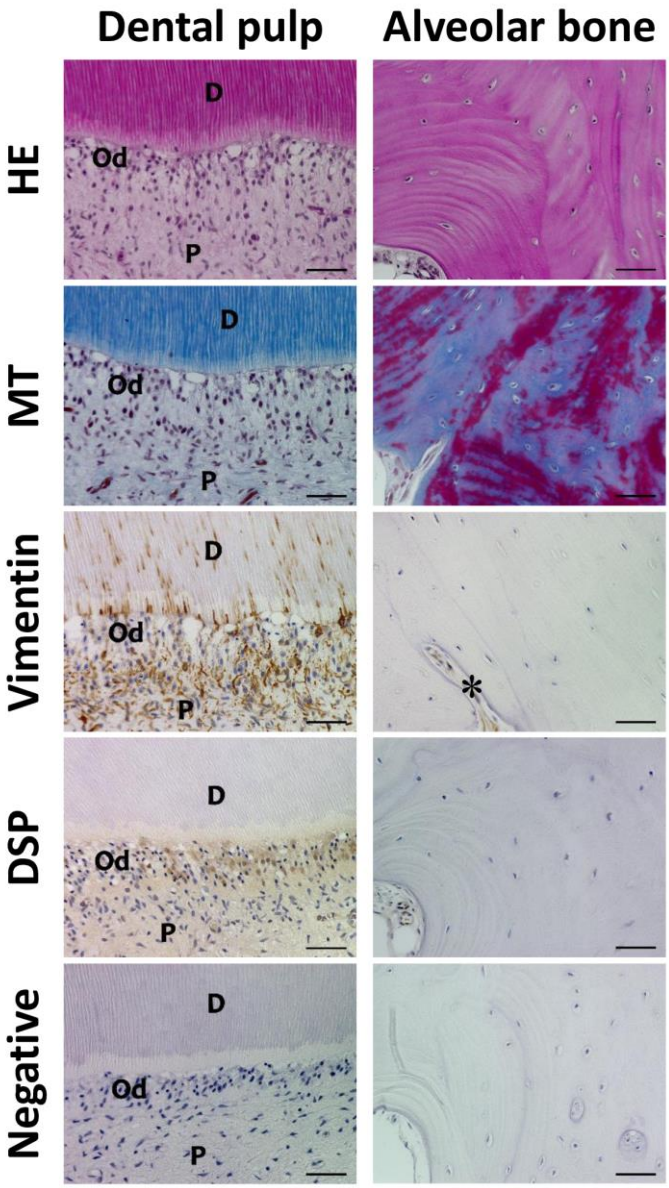

Additional file 4: Fig. S3

Histological and immunohistochemical examination of native dental pulp and alveolar bone. HE and MT staining. Scale bars, 50 μm. * denotes bone marrow. DSP, dentin sialoprotein. D, dentin; P, dental pulp; Od, odontoblasts.

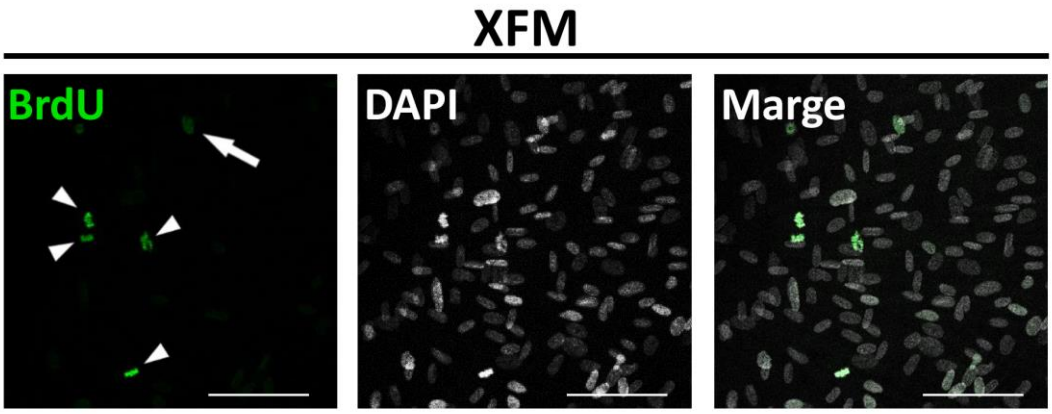

Additional file 5: Fig. S4

BrdU staining of over-confluent XFM cultures on day 14 post-seeding. Arrow indicates BrdU-positive oval nucleus. Arrowheads indicate BrdU-positive condensed nuclei. Scale bars, 100 μm.

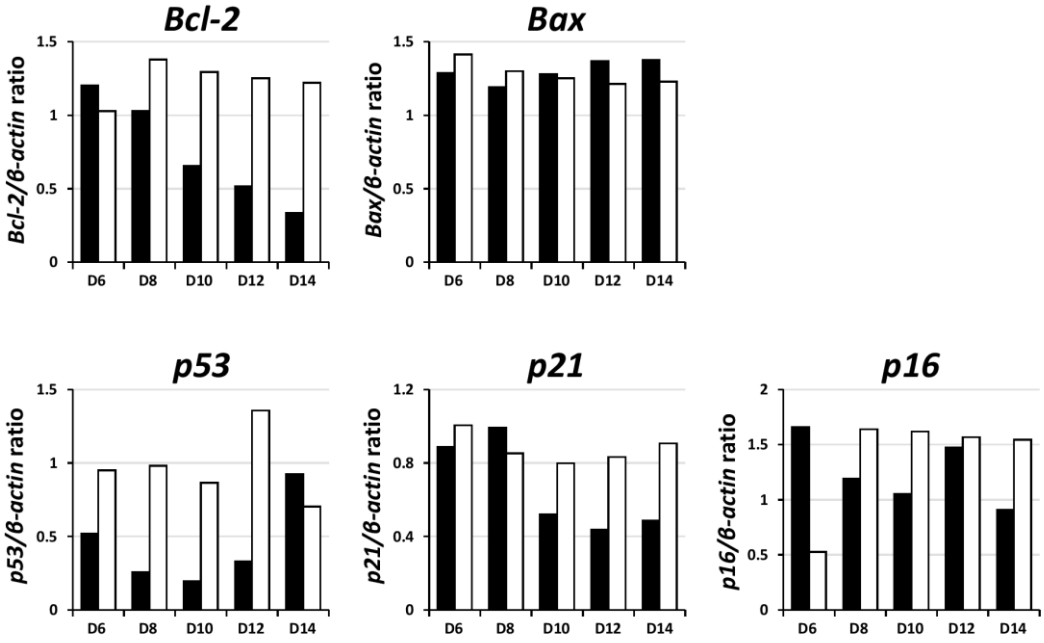

Additional file 6: Fig. S5

Semiquantitative densitometric analysis of the corresponding results of RT-PCR indicated in Fig. 5f. The time-course gene-expression profile for apoptosis and cell cycle regulators during cell-growth evaluation in DPSCs cultured in XFM (black columns) and SCM (white columns). The observed signals are expressed as a ratio to β-actin signal intensity for the respective genes.

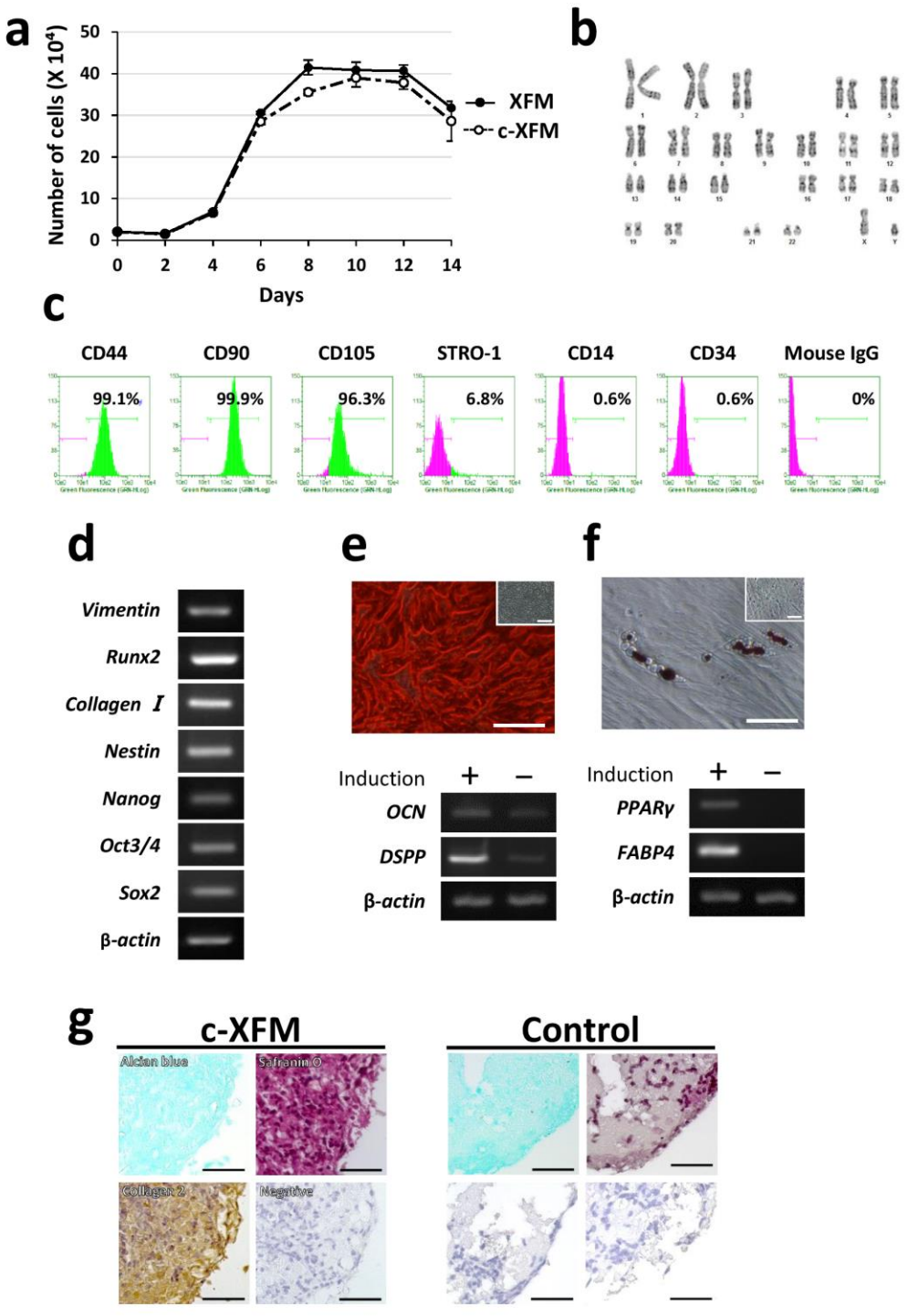
a
Number of cells (X 10⁴)
50
40
30
20
10
0
0 2 4 6 8 10 12 14
Days
XFM
c-XFM
b
c
CD44
CD90
CD105
STRO-1
CD14
CD34
Mouse IgG
99.1%
99.9%
96.3%
6.8%
0.6%
0.6%
0%
d
Vimentin
Runx2
Collagen I
Nestin
Nanog
Oct3/4
Sox2
β-actin
e
Induction + –
OCN
DSPP
β-actin
f
Induction + –
PPARγ
FABP4
β-actin
g
c-XFM
Control
Alcian blue
Safranin O
Collagen 2
Negative

Additional file 7: Fig. S6

Stem cell characterization of cryopreserved DPSCs cultured in xenogeneic serum-free culture medium (c-XFM). **a** Growth-curve evaluation of c-XFM cells and non-cryopreserved XFM cells at passage 3 during 14 days of culture. No statistically significant differences were observed in cell growth during the 14 days post-seeding. **b** A normal karyotype was maintained in c-XFM cells at passage 10. **c** Flow cytometry for cell-surface markers of MSCs and hematopoietic cells on c-XFM cells. **d** Gene-expression profile of MSC and osteo/odontogenic markers in c-XFM cells as determined by RT-PCR. **e** Alizarin red staining (ALZ) and RT-PCR results for osteo/odontogenic marker genes from mineral-inducing cultures of c-XFM cells after a 4-week induction (+) or 4 weeks without induction (−). Insets in ALZ images show no-induction cultures (4 weeks). Scale bars, 100 μm. **f** Oil red O-staining (ORO) showing lipid droplets and RT-PCR results for adipogenic marker genes (−) in c-XFM cells after a 4-week adipogenic induction (+) or 4 weeks without induction. Insets in ORO images showing no-induction cultures (4 weeks). Scale bars, 50 μm. **g** Alcian blue, Safranin O, and immunohistochemical staining showing chondrogenic induction cultures of c-XFM cells after 4 weeks. No chondrogenic induction after 4 weeks (control). Scale bars, 50 μm. Collagen 2, type II collagen.

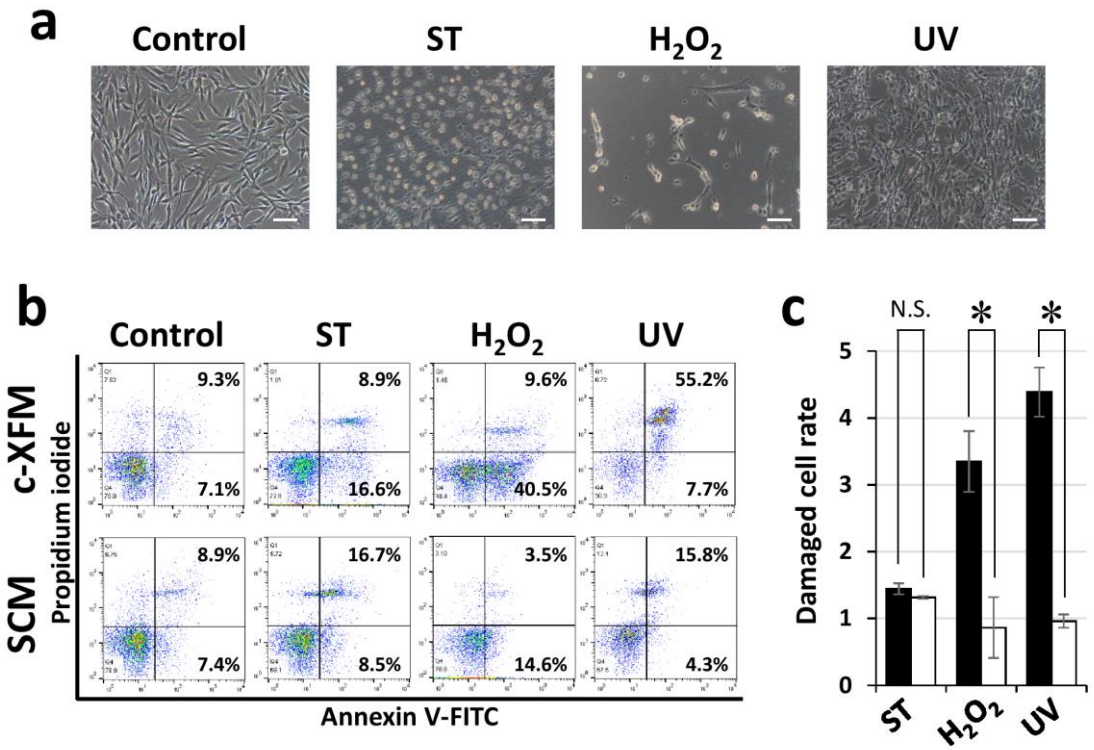

Additional file 8: Fig. S7

In vitro assessment of cellular stress/damage of cryopreserved DPSCs induced by extrinsic cytotoxic stimuli under xenogeneic serum-free culture medium (c-XFM). **a** Degenerative morphological changes of c-XFM cells before (control) and after treatment with staurosporine (ST), H_2O_2, or UV radiation. Scale bars, 100 μm. **b** Flow-cytometric analysis of cytotoxic stimulus-treated c-XFM cells and DPSCs cultured in SCM using an Annexin V/PI system and **c** quantification of the damaged cells in c-XFM (black columns) and SCM (white columns) cultures. *$P < 0.01$. N.S., no significant difference.

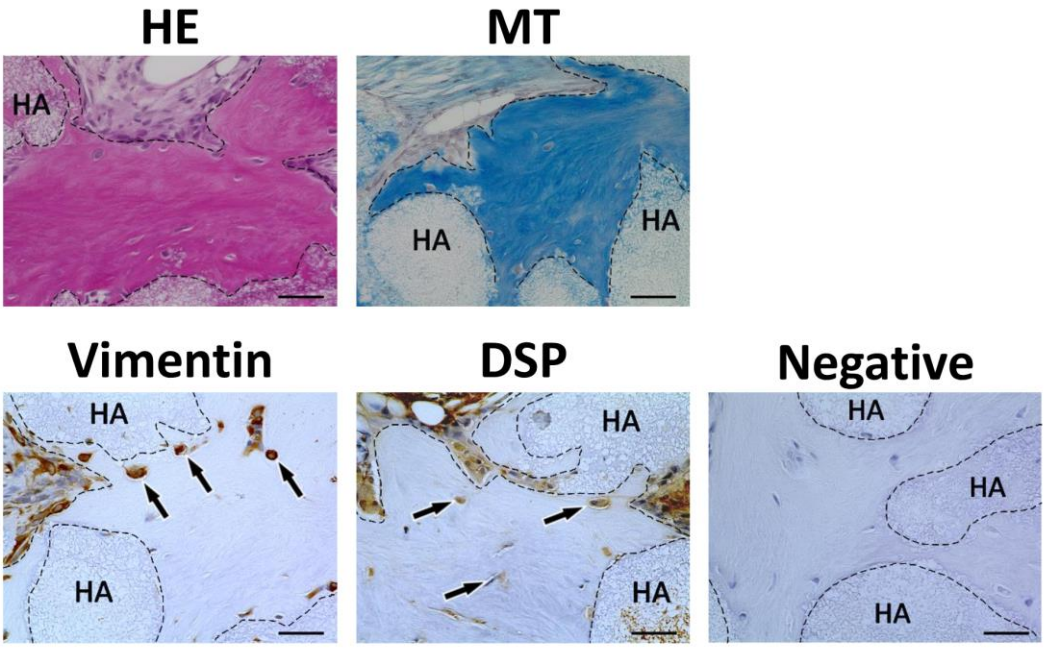

Additional file 9: Fig. S8

In vivo subcutaneous transplantation of *ex vivo*-expanded cryopreserved DPSCs cultured in xenogeneic serum-free culture medium (c-XFM). HA scaffolds containing c-XFM cells were histologically evaluated by HE, MT, and immunohistochemical staining 16 weeks after transplantation. DSP, dentin sialoprotein. Arrows indicate cells embedded within the newly formed hard tissue, which is outlined by dashed lines. The primary antibody was omitted during immunostaining (negative control). Scale bars, 50 μm.

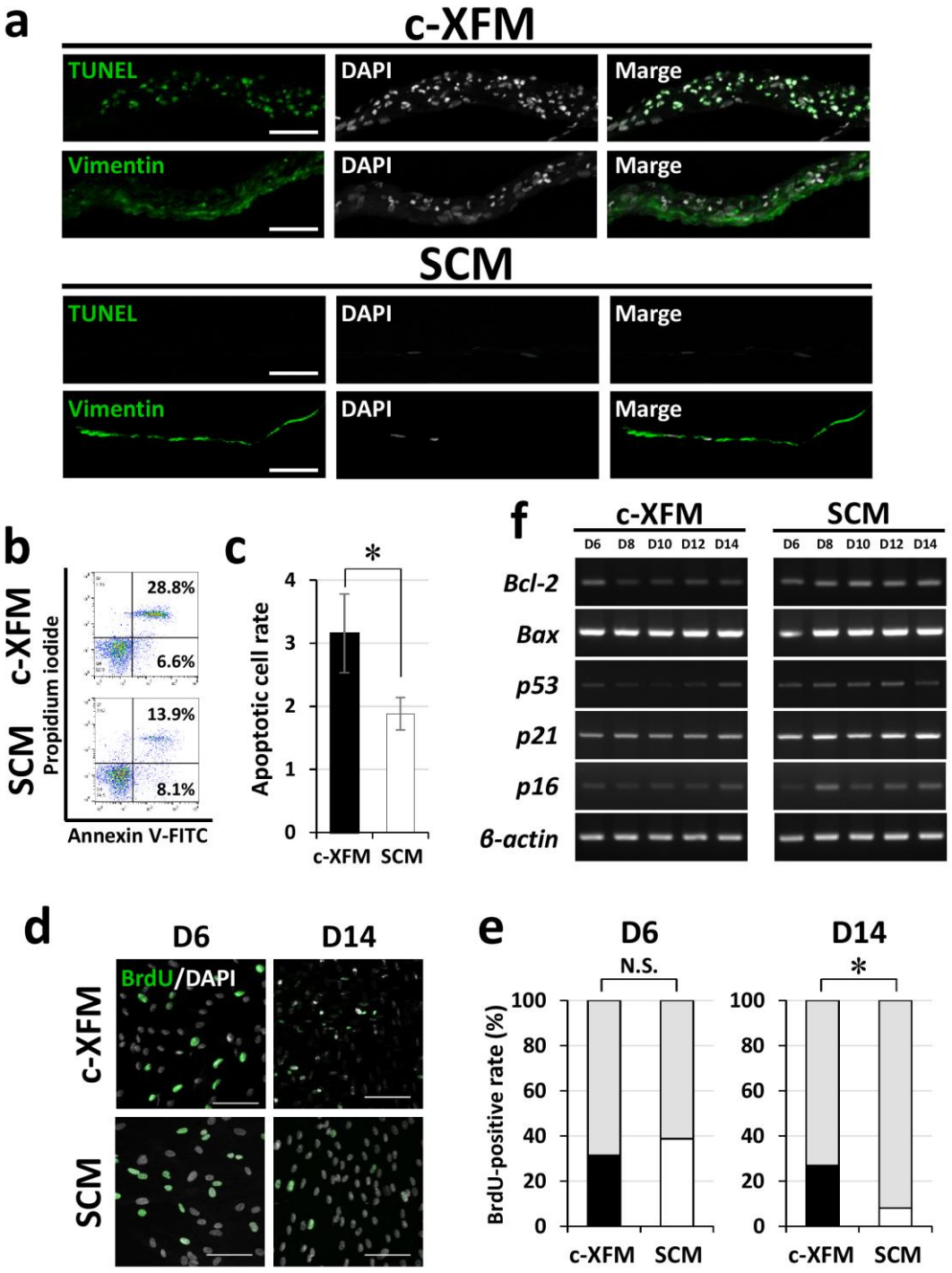
a
c-XFM
TUNEL
DAPI
Marge
Vimentin
DAPI
Marge
SCM
TUNEL
DAPI
Marge
Vimentin
DAPI
Marge
b
c-XFM
SCM
Propidium iodide
28.8%
6.6%
13.9%
8.1%
Annexin V-FITC
c
Apoptotic cell rate
*
0
1
2
3
4
c-XFM
SCM
f
c-XFM
SCM
D6 D8 D10 D12 D14
D6 D8 D10 D12 D14
Bcl-2
Bax
p53
p21
p16
β-actin
d
D6
D14
c-XFM
SCM
BrdU/DAPI
e
D6
D14
N.S.
*
BrdU-positive rate (%)
0
20
40
60
80
100
c-XFM
SCM
c-XFM
SCM

Additional file 10: Fig. S9

Cellular behavior of cryopreserved DPSCs at over-confluence under xenogeneic serum-free culture medium (c-XFM). **a** TUNEL staining was positively visualized in c-XFM cells, but not in DPSCs cultured in SCM, whereas both cell types were positively immunostained for vimentin. Scale bars, 100 μm. **b** Flow-cytometric analysis using an Annexin V/PI system indicated that the number of apoptotic cells in over-confluent c-XFM cultures was higher than those in SCM cultures, and **c** quantification of the apoptotic cells demonstrated a statistically significant difference between cell types. *$P < 0.01$. **d** BrdU uptake in over-confluent c-XFM cultures on day 14 was comparable to that on day 6, whereas it was decreased in SCM cells at this time point. **e** Quantification of BrdU-positive cells in c-XFM and SCM cultures statistically supported the results in **d**. Scale bars, 100 μm. *$P < 0.01$. **f** Time-course gene-expression profile for apoptosis and cell cycle regulators during cell-growth evaluation of c-XFM cells was comparable to that in XFM cells according to RT-PCR analysis (see Fig. 5f). N.S., no significant difference.

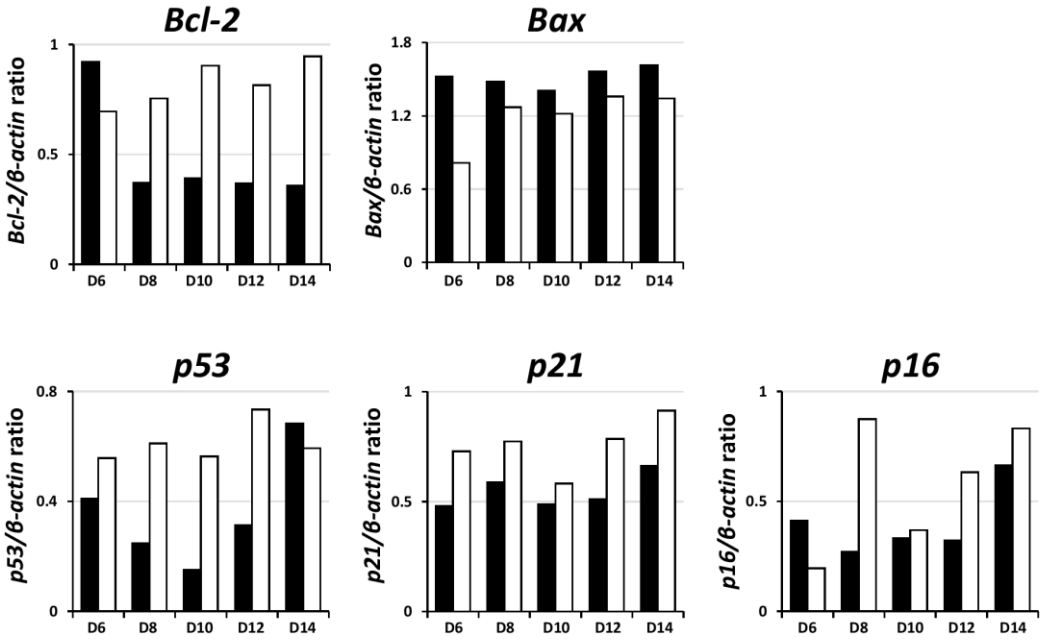

Additional file 11: Fig. S10

Semiquantitative densitometric analysis of the RT-PCR results from Fig. S9f. Time-course gene-expression profile for apoptosis and cell cycle regulators during cell-growth evaluation in c-XFM (black columns) and SCM (white columns) cultures. The observed signals are expressed as a ratio to β-actin signal intensity of the respective genes. The expression pattern in c-XFM cells was comparable to that in XFM cells (see Fig. 5f).

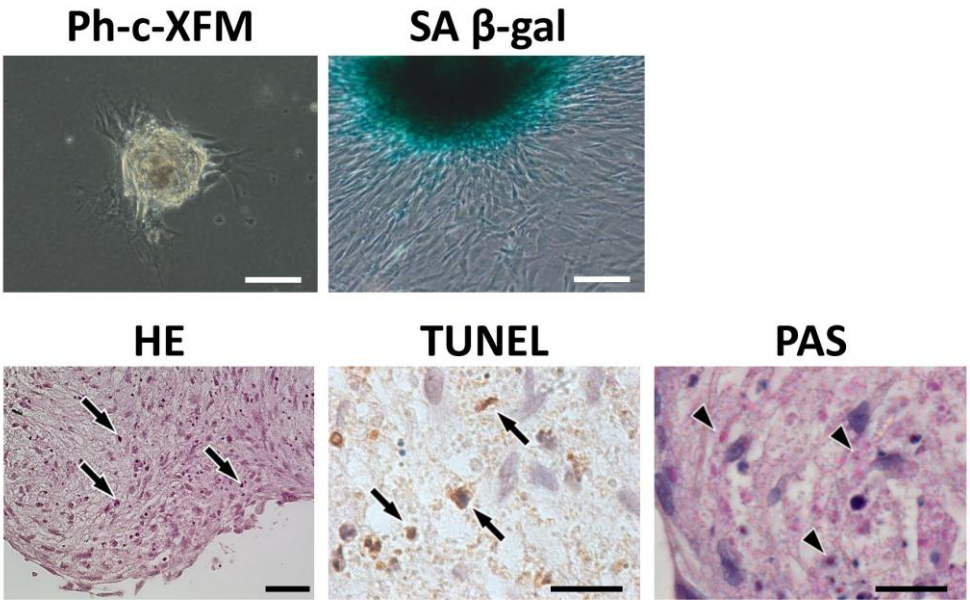

Additional file 12: Fig. S11

Cellular-behavioral analysis after subculture of over-confluent cryopreserved DPSCs cultured in xenogeneic serum-free culture medium (c-XFM). Phase-contrast image of subcultured over-confluent, multilayered c-XFM cells (Ph-c-XFM). Scale bar, 50 µm. Positive SA β-gal staining of a cell aggregate derived from subcultured over-confluent c-XFM cells (SA β-gal). Scale bar, 50 µm. Histological evaluation of a cell aggregate by HE, TUNEL, and PAS staining of the cell aggregate. Arrows indicate condensed nuclei according to HE staining (scale bar, 50 µm) and TUNEL-positive cells (scale bar, 20 µm). Arrowheads indicate PAS-positive lipofuscin granules. Scale bar, 20 µm.

Table 1. Primer sequences and amplification conditions for RT-PCR analysis

Gene	Primer sequences, 5' to 3'	Product size (bp)	Annealing temp. (°C)	PCR cycles	GenBank accession number
Vimentin	S: GGGACCTCTACGAGGAGGAG	200	55	35	NM_003380
	A: CGCATTGTCAACATCCTGTC				
Runx2	S: CCCCACGACAACCGCACCAT	292	55	35	NM_004348
	A: GTCCACTCCGGCCCACAAATC				
Collagen I	S: CCAAATCTGTCTCCCCAGAA	214	55	35	NM_000088
	A: TCAAAAACGAAGGGGAGATG				
Nestin	S: AACAGCGACGGAGGTCTCTA	220	55	35	NM_006617
	A: TTCTCTTGTCCCGCAGACTT				
Nanog	S: ACCTTCCAATGTGGAGCAAC	199	55	35	NM_024865
	A: GAATTTGGCTGGAACTGCAT				
Oct3/4	S: GACAGGGGGAGGGGAGGAGCTAGG	144	60	35	NM_001173531
	A: CTTCCCTCCAACCAGTTGCCCCAAAC				
Sox2	S: AACCCCAAGATGCACAACTC	152	60	40	NM_003106
	A: CGGGGCCGGTATTTATAATC				
OCN	S: GCTGAGTCCTGAGCAGCAG	323	60	30	NM_199173
	A: CGATAGGCCTCCTGAAAGC				
DSPP	S: CATTTGGGCAGTAGCATGGG	170	55	35	NM_014208
	A: CACCTTCATGCACCAGGACA				
PPARγ	S: TCGGATCCCTCCTCGGAAAT	399	60	35	AB565476
	A: GCAGGCTCCACTTTGATTGC				
FABP4	S: TGGGCCAGGAATTTGACGAA	212	60	35	NM_001442
	A: ACGTCCCTTGGCTTATGCTC				
Bcl-2	S: GGTGAACTGGGGGAGGATTG	214	60	35	NM_000633
	A: GAAATCAAACAGAGGCCGCA				
Bax	S: AAGAAGCTGAGCGAGTGTCTC	338	60	35	NM_001291428
	A: AGTCGCTTCAGTGACTCGG				
p53	S: TACCAGGGCAGCTACGGTTT	572	55	25	AB082923
	A: CCTTTCTTGCGGAGATTCTCT				
p21	S: TCAGAACCGGCTGGGGATGT	554	60	35	NM_001291549
	A: AGATGTAGAGCGGGCCTTTG				
p16	S: CCCAACGCACCGAATAGT	135	65	35	XM_011517676
	A: CACGGGTCGGGTGAGAGT				
β-actin	S: GGACTTCGAGCAAGAGATGG	234	60	30	NM_001101
	A: AGCACTGTGTTGGCGTACAG				

Runx2, Runt-related transcription factor 2; Oct3/4, POU class 5 homeobox 1 (POU5F1); SOX2, Sex determining region Y-box 2; OCN, Osteocalcin; DSPP, Dentin sialophosphoprotein; PPARγ, Peroxisome proliferator-activated receptor γ; FABP4, Fatty acid binding protein 4; Bcl-2, B-cell lymphoma 2; BAX, B-cell lymphoma-2 associated X.